

For Reference

NOT TO BE TAKEN FROM THIS ROOM

Ex LIBRIS
UNIVERSITATIS
ALBERTAENSIS



THE UNIVERSITY OF ALBERTA

FLEXURAL AND LATERAL-TORSIONAL BUCKLING
STRENGTHS OF DOUBLE ANGLE STRUTS

BY



NORMAN JAMES NUTTALL

A THESIS

SUBMITTED TO THE FACULTY OF GRADUATE STUDIES
IN PARTIAL FULFILMENT OF THE REQUIREMENTS
FOR THE DEGREE OF MASTER OF SCIENCE

DEPARTMENT OF CIVIL ENGINEERING

EDMONTON, ALBERTA

FALL, 1970

Thesis
1970 F
199

UNIVERSITY OF ALBERTA
FACULTY OF GRADUATE STUDIES

The undersigned certify they have read, and recommend to the Faculty of Graduate Studies for acceptance, a thesis entitled FLEXURAL AND LATERAL-TORSIONAL BUCKLING STRENGTHS OF DOUBLE ANGLE STRUTS submitted by NORMAN JAMES NUTTALL in partial fulfilment of the requirements for the degree of Master of Science.

ABSTRACT

This investigation attempts to define the flexural and lateral-torsional buckling strengths of double angle struts.

CSA-G40.12 steel was used to establish the basic material properties. Residual stress measurements were performed on specimens cut from five different angle shapes. The results are reported herein along with the results of tension tests on comparison specimens.

The residual stress distribution was idealized and used as input for a computer program which computed the flexural and lateral-torsional buckling strengths based on the tangent modulus concept. Column curves were developed for several different column sections to investigate the influence of member asymmetry, leg thickness, angle separation, yield stress level and residual stress distribution.

For the double angle members, the lateral-torsional buckling strength coincided (within 2%) with the (fictitious) y-y axis buckling strength for all cases investigated. Thus the traditional design which ignores the possibility of lateral-torsional buckling may be used with confidence for these members.

ACKNOWLEDGEMENTS

This study is part of an investigation "Lateral-Torsional Buckling of Thin Open Walled Sections" in progress at the Department of Civil Engineering, University of Alberta, P.F. Adams is the project Director. The project is sponsored financially by the Canadian Steel Industries Construction Council with technical assistance from the Canadian Institute of Steel Construction.

The assistance of Mr. A.J.M. Aikman, Alberta Regional Engineer, CISC, and Mr. H.A. Krentz, Chief Administrative Engineer, CISC, is particularly acknowledged. The financial support to the author in the form of a CISC scholarship provided by the Alberta Regional Committee of the CISC is also gratefully acknowledged.

The author wishes to express his sincere appreciation to P.F. Adams who directed the work and whose advice and continuing guidance were extremely valuable.

The comments and criticisms of G.L. Kulak and J.S. Kennedy who served on the thesis committee, are gratefully acknowledged.

The contributions of H. Panse, J. McLean and their respective staffs, along with D. Delicate and D. Chambers in completing the testing program and Miss H. Wozniuk and Mrs. P. Brunel who typed the report are also acknowledged.

TABLE OF CONTENTS

	Page
Title Page	i
Approval Sheet	ii
Abstract	iii
Acknowledgements	iv
Table of Contents	v
List of Tables	vi
List of Figures	vii
CHAPTER I INTRODUCTION	1
CHAPTER II PREVIOUS INVESTIGATIONS	8
CHAPTER III MATERIAL PROPERTIES	20
CHAPTER IV ANALYTICAL INVESTIGATION	34
CHAPTER V TEST PROGRAM AND RESULTS	40
CHAPTER VI APPLICATIONS TO DESIGN	63
CHAPTER VII SUMMARY AND CONCLUSIONS	71
NOMENCLATURE	73
LIST OF REFERENCES	75
APPENDIX A	77

LIST OF TABLES

Table		Page
1.1	Standard Gauge Distances for Angles	7
3.1	Chemical Composition and Mill Test Results	29
3.2	Material Properties	30
3.3	Residual Stress Distribution	33
5.1	Critical Stresses	62
6.1	Factors of Safety	70

LIST OF FIGURES

Figure	Page
1.1 Double Angle Struts	4
1.2 Buckling Strength of Compression Member	5
1.3 Modes of Buckling for Double Angle Struts	6
2.1 Column Equilibrium Positions	17
2.2 Buckling Deformations	18
2.3 Residual Stress Distribution-Single Angle	19
2.4 Residual Stress Values	19
3.1 Residual Stress Measurements	23
3.2 Comparison of Residual Stress Distributions (4 x 4 x 3/8") Angle	28
4.1 Stress-Strain Curve	37
4.2 Strain Patterns	37
4.3 Double Angle Connection at Gauge Location	38
4.4 Flow Chart for Computer Program	39
5.1 Influence of Member Asymmetry	46
5.2 Influence of Leg Thickness	51
5.3 Influence of Leg Separation	56
5.4 Influence of Yield Stress	57
5.5 Influence of Residual Stress	61
6.1 Ultimate and Design Curves Flexural Buckling	68
6.2 Ultimate and Design Curves Lateral-Torsional Buckling	69

CHAPTER I

INTRODUCTION

Double angles are commonly used in building structures as compression members in trusses and as bracing members to ensure the stability of the structure. These members are normally considered to be loaded axially, as the secondary bending moments, induced by the connections, are small¹⁵.

A typical building panel is shown in Figure 1.1. The double angles are used as diagonal bracing members and may be designed to act only in tension, or to resist both tensile and compressive forces. The angles forming a member are separated by the thickness of the gusset plate (to facilitate connection) and are either bolted or welded to the connection plate. A typical bolted connection is shown in Figure 1.1(b) and the corresponding welded detail in Figure 1.1(c). The angles are connected at intervals along their lengths so that the two angles act as a single unit. The end restraint offered by the usual type of connection is small¹⁵. Thus in design, it is assumed that the member acts as a pin-ended column having an effective length equal to the distance between the extremities of the two connections.

The range of angles sizes used in building structures generally varies from the very small ($3 \times 2\frac{1}{2} \times \frac{3}{16}$ ") to the larger size ($8 \times 8 \times 1\frac{1}{8}$ "), with a selection of equal and unequal leg sizes available between these

limits. The length of the angle leg governs the location of the bolts in the connection. Standard gauge distances are used as shown in Table 1.1, with g representing the gauge distance for a single line of bolts and g_1 and g_2 denoting the gauge distance if two lines of bolts are used. The use of welded connections as shown in Figure 1.1(c) is also common with the leg thickness governing the size and strength of the weld⁵.

The ultimate strength of a compression member is usually assumed to be equal to its buckling strength; defined as the load at which the member can exist in two adjacent equilibrium positions. Figure 1.2 shows a schematic column curve which plots the applied stress corresponding to the buckling load, σ , non-dimensionalized by the yield stress, σ_y , versus the slenderness ratio (L/r), where L represents the member length and r the radius of gyration.

The branch E-D-B-C of the curve represents the relationship between the critical applied stress, σ , and the slenderness ratio when buckling occurs before yielding of any fibre of the cross-section. For an elastic-perfectly plastic material this curve would remain valid until the value of σ reaches the yield stress, σ_y , of the material. For smaller values of L/r , the critical stress would remain at σ_y thus defining the branch A-D-B-C.

Residual stresses caused by the hot rolling and cooling process, cause sections of the cross-section to yield at stresses below σ_y . This produces a deviation from the elastic-perfectly plastic curve, at a

stress level equal to yield stress minus the maximum residual stress, σ_r , as shown by the curve A-B-C. As the load is increased parts of the cross-section yield before buckling occurs. For smaller values of L/r , larger portions of the cross-section yield before buckling until finally the entire cross-section is yielded at $\sigma/\sigma_y = 1.0$.

Buckling of doubly symmetric sections may occur in any one of three independent modes; flexural buckling about either of the two principal axes or torsional buckling. Double angle struts have only a single axis of symmetry, however, and thus there exist only two independent modes; flexural buckling about a principal axis, or a combination of torsional buckling and flexural buckling about the other principal axis (lateral-torsional buckling) as shown in Figure 1.4.

The present investigation attempts to define both the flexural and lateral-torsional buckling strengths of double angle struts. The results will be compared with design provisions with the aim of determining the factors of safety inherent in the various procedures.

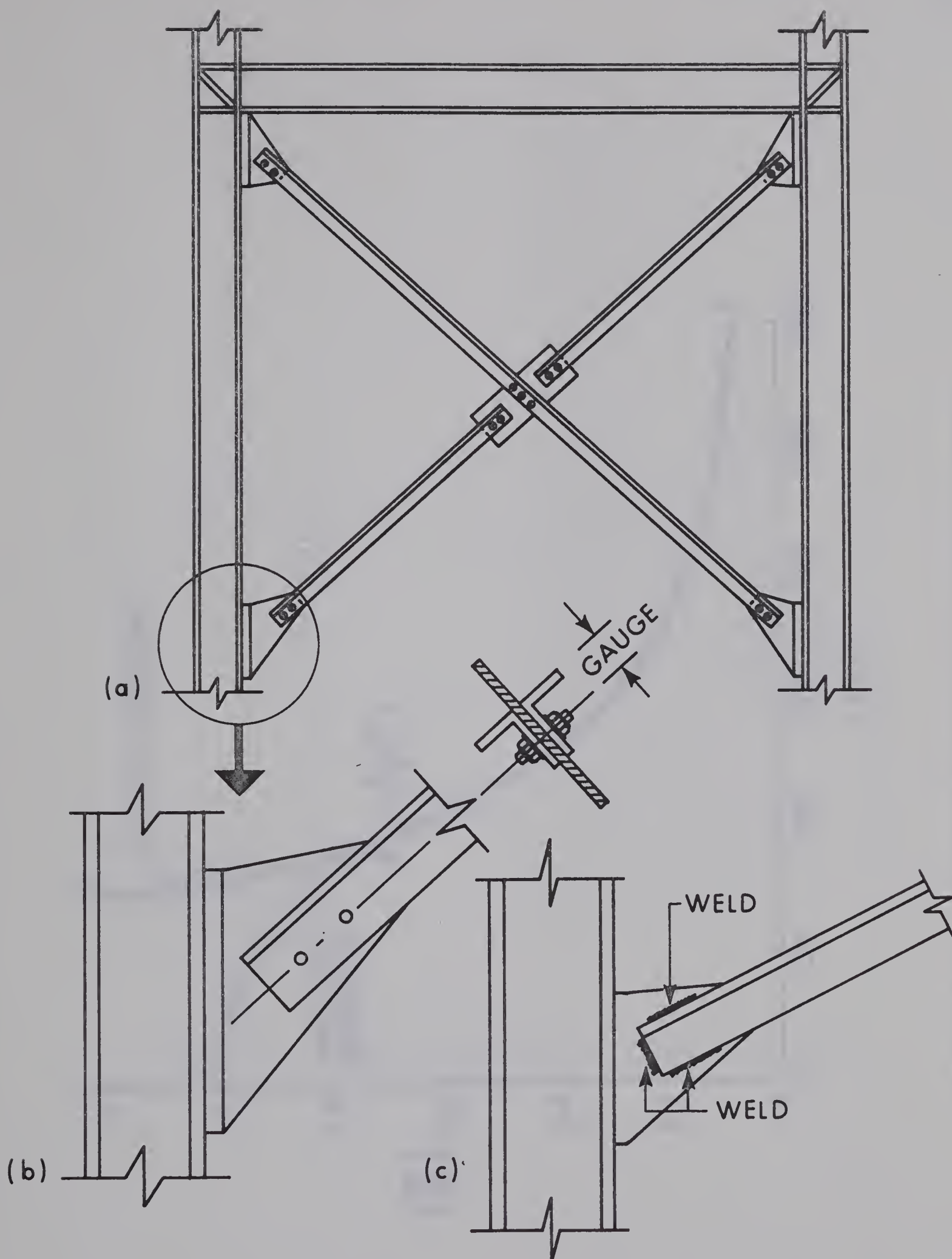


Figure 1.1 Double Angle Struts

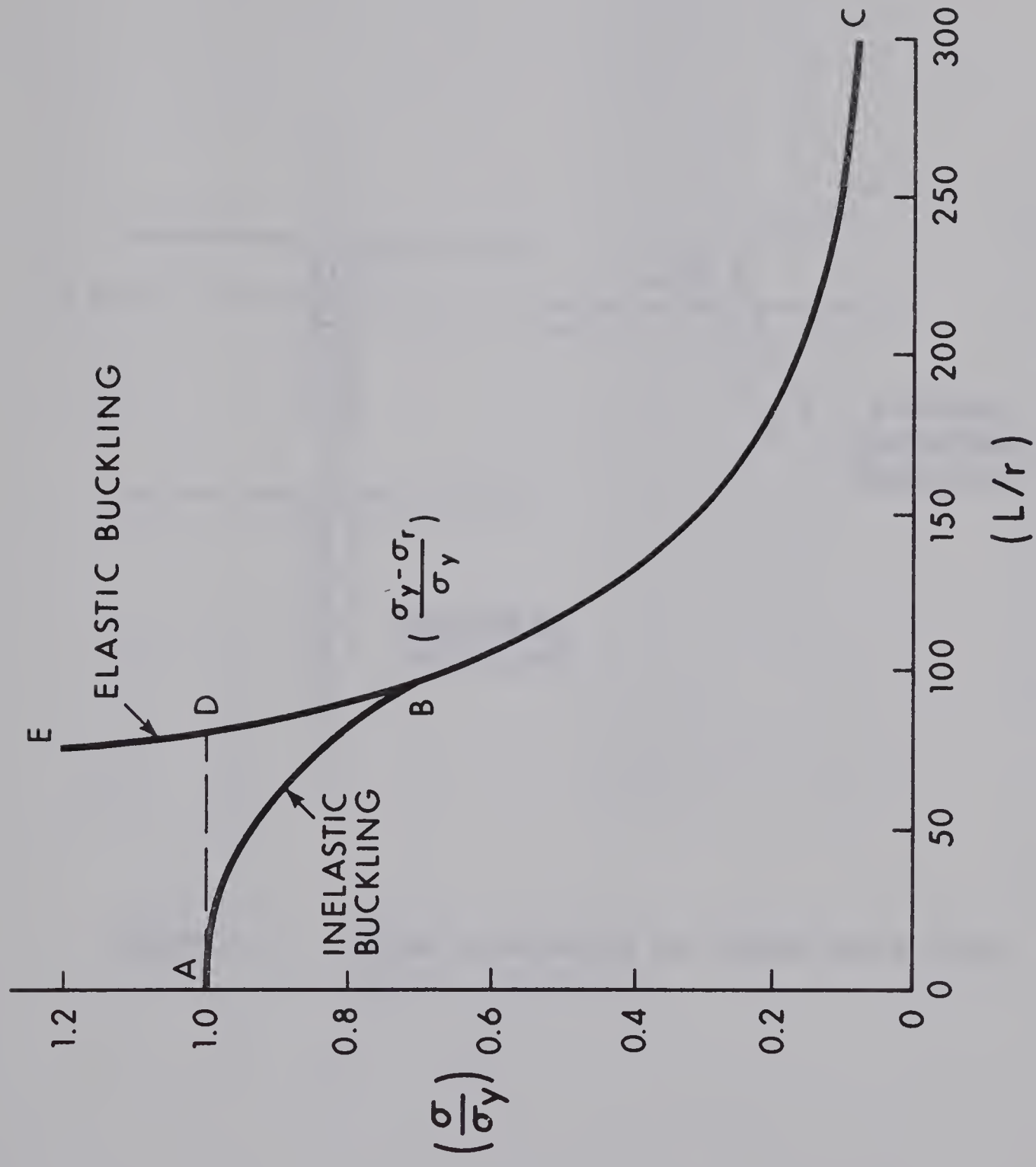


Figure 1.2 Buckling Strength of Compression Member

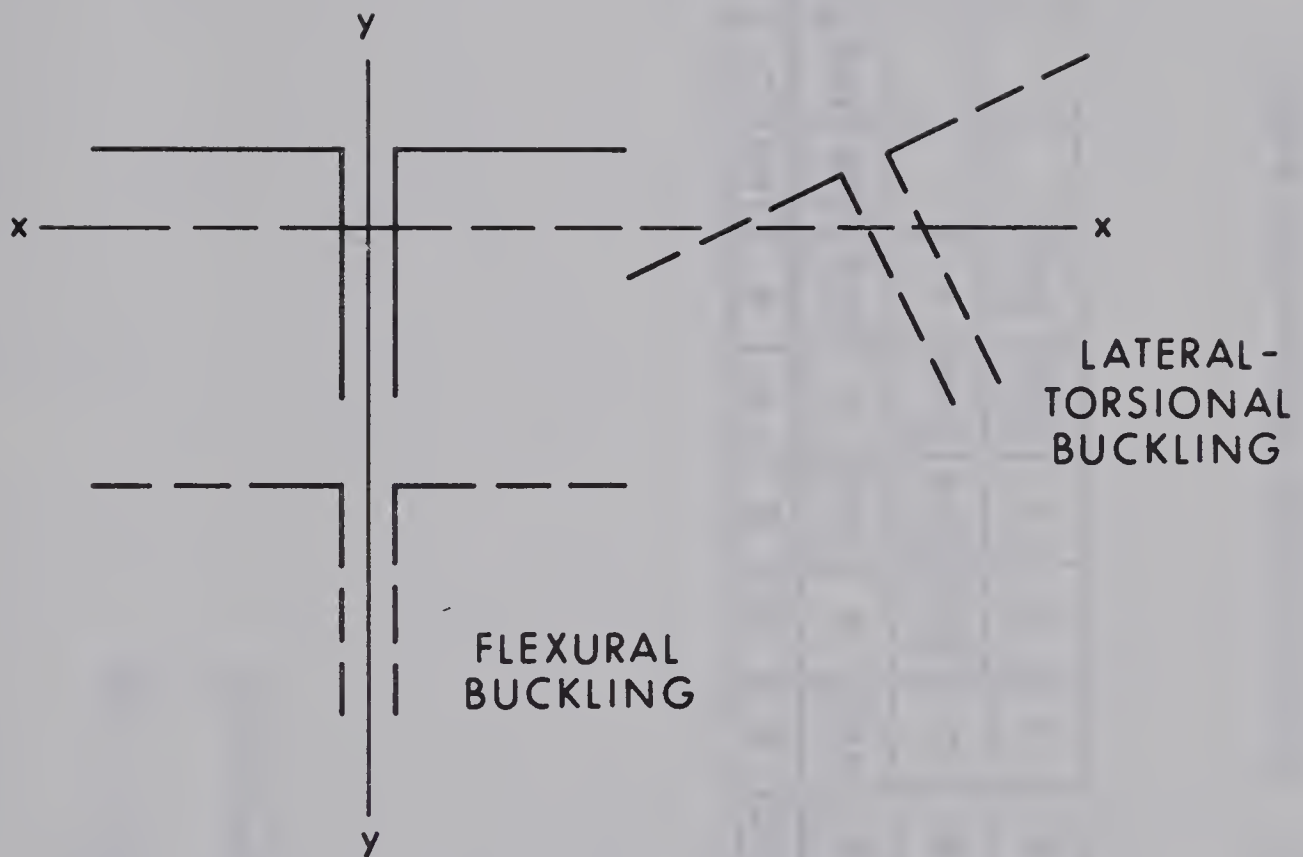
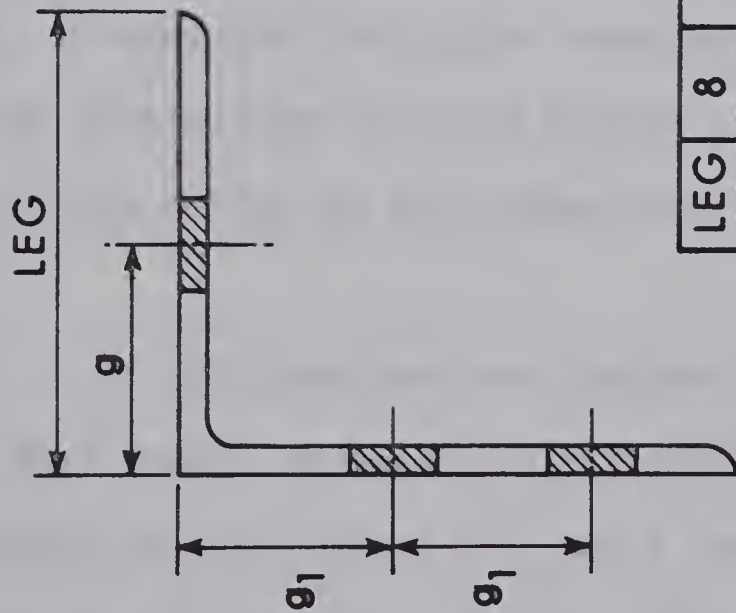


Figure 1.3 Modes of Buckling for Double Angle Struts



LEG	8	7	6	5	4	3 1/2	3	2 1/2	2	1 1/2	1
g	4 1/2	4	3 1/2	3	2 1/2	2 1/4	1 3/4	1 3/8	1 1/8	7/8	5/8
g ₁	3	2 1/2	2 1/2	2 1/4	2	-	-	-	-	-	-
g ₂	3	3	3	2 1/2	1 3/4	-	-	-	-	-	-

Table 1.1 Standard Gauge Distance for Angles

CHAPTER II

PREVIOUS INVESTIGATIONS

The solution to the differential equation, which expresses the equilibrium of the member in the deformed position (Figure 2.1) was first obtained by Euler in 1759¹⁰. The solution defines the load at which a slender, axially loaded column of uniform cross-section can exist in either a straight or slightly deformed configuration. The solution is limited to slender columns in which the strain at the instant of buckling does not exceed the yield strain.

Most practical columns do not fall within the range of applicability of the Euler solution and in 1889 Engesser¹⁰ developed the first inelastic buckling theory. This, the original tangent modulus theory, assumed that the column remained straight until the buckling load was attained and that the modulus of elasticity associated with the buckling motion was the tangent modulus at the critical stress level.

In 1895 Considère and Jasinski challenged this theory on the basis that lateral deflection would produce additional loading (due to bending) on the concave side and a corresponding unloading on the convex side. In the light of this criticism Engesser modified his original thinking and postulated the reduced modulus theory, wherein the tangent modulus was applied to only the loading portion of the

cross-section and the original elastic modulus was used to determine the stiffness of the unloading portion. Tests conducted by von Kármán in 1910, however, agreed well with the original tangent modulus theory¹⁰.

The difference between the two concepts remained unresolved until 1947. From the results of careful model tests Shanley¹⁹ showed that an initially straight column will buckle at the tangent modulus load, then continue to deform with increasing load. Shanley concluded that for an initially straight column, the tangent modulus load is a lower bound on the ultimate strength of the column and that the reduced modulus load gives an upper bound for the ultimate strength, if the column is temporarily supported beyond the tangent modulus load. The ultimate strength of an actual column lies between the tangent modulus and reduced modulus load, with the tangent modulus being a reasonable estimate of the strength for structural steel members. The results of Shanley's work led to a reinstatement of the tangent modulus theory, and to additional applications of the basic concept, in that strain reversals of previously yielded fibres are ignored in computing the buckling strength.

Residual stresses affect column strength in that the "effective" stress-strain curve for the complete cross-section is entirely different from the stress-strain curve obtained from a coupon taken from the material. In preparing tensile coupons for testing, residual stresses are at least partially released and the stress-strain curve approaches the idealized elastic-plastic curve. To assess

the magnitude of the residual stresses, stub column tests on the complete cross-section have been used⁹. In a stub column the residual stresses cause individual fibres to yield well below the attainment of the yield load for the specimen. The yielded fibres offer no resistance to additional loading and thus the load-deflection (stress-strain) curve deviates from the original (elastic) straight line. The stress at the point of deviation then can be used as a crude indication of the maximum compressive residual stress. The alternative to this procedure is to determine the distribution of residual stresses using a sectioning procedure. The use of the tangent modulus theory is equivalent to computing the flexural stiffness of the member based on the elastic core of the cross-section at buckling⁴. The critical stress level can then be formulated as

$$\sigma_c = \frac{\pi^2 E I_e}{A L^2} \quad (2.1)$$

where E , represents the modulus of elasticity and I_e is the moment of inertia of the elastic core. The cross-sectional area is represented by A while L denotes the length of the column.

The basic equations for both flexural and torsional buckling have been derived for doubly symmetric sections and have been solved for the buckling strength of the member in both the elastic and inelastic ranges. Lee et al¹⁶ have reported the results of an analytical study of the buckling strength of wide flange sections. In this study the

influence of the residual stress distribution on the torsional buckling strength is reported. Three conditions must be satisfied by the residual stress distribution in order that the member is in equilibrium before the load is applied. The net axial force acting on the member must be equal to zero; this implies that:

$$\int_A \sigma_r dA = 0 \quad (2.2)$$

In addition the bending moments about the x and y axes must vanish; this implies that both:

$$\int_A \sigma_r x dA = 0 \quad (2.3)$$

and

$$\int_A \sigma_r y dA = 0 \quad (2.4)$$

Lee also requires that the residual stress distribution produce no twisting moment with respect to the shear centre for any small deformation. Thus

$$\int_A \sigma_r (x_0^2 + y_0^2) dA = 0 \quad (2.5)$$

where x_0 and y_0 represent the location of the shear centre. If this fourth condition is satisfied, there will be no reduction in the

torsional buckling load due to residual stresses, except that reduction associated with the gradual deterioration of the cross-section.

It has been shown¹² that Equation 2.5 is not a necessary condition for equilibrium of the residual stresses and in fact, measured distributions do not satisfy this condition. This implies that the presence of residual stresses will reduce the torsional buckling strength somewhat and must be considered.

The deformations at the instant of (flexural-torsional) buckling, for singly symmetric sections, involve a translation, u , in the x -direction as shown in Figure 2.2 and a rotation, ϕ , about the shear centre. Pure flexural buckling of the same section involves only a translation in the y -direction v . Chajes and Winter⁶ have summarized the three equilibrium equations for a singly symmetric section in the deformed condition as:

$$EI_y u^{IV} + P(u^{II} + y_0 \phi^{II}) = 0 \quad (2.6)$$

$$EI_x v^{IV} + P(v^{II}) = 0 \quad (2.7)$$

$$EI_w \phi^{IV} - (GK_T + \bar{K})\phi^{II} + Py_0 u^{II} = 0 \quad (2.8)$$

where I_x and I_y are the moments of inertia about the principal axes. I_w represents the torsion constant for warping and K_T the St. Venant torsion constant. The deformations are given by u , v and ϕ (Figure 2.2)

and the primes represent differentiation with respect to the co-ordinate measured along the longitudinal axis. The axial load P is given by

$\int_A \sigma dA$ and \bar{K} is defined as $\int_A \sigma a^2 dA$ where a represents the distance from a point on the cross-section to the shear centre.

In the derivations of equations 2.6 to 2.8 it was assumed that the deformations were small and that the material was elastic. Solutions to these equations lead to the two buckling loads for the member. For a column with ideally pinned boundary conditions at both $z = 0$ and $z = L$;

$$u = v = \phi = 0$$

and

$$u'' = v'' = \phi'' = 0$$

The equations result in the following solution:

$$-\frac{\bar{K}}{P} (P - P_y)(P - P_x)(P - P_\phi) - P^2 y_0^2 (P - P_x) = 0 \quad (2.9)$$

where

$$P_y = \frac{\pi^2 EI_y}{L^2} \quad (2.10)$$

$$P_x = \frac{\pi^2 EI_x}{L^2} \quad (2.11)$$

and

$$P_\phi = -\frac{P}{\bar{K}} \left[GK_T + \frac{\pi^2 EI_w}{L^2} \right] \quad (2.12)$$

Equation 2.9 has two solutions, $P = P_x$ which represents pure flexural buckling and $P_{\phi y}$ equal to the lower root of the quadratic resulting from the remainder of Equation 2.9. This load represents the coupled flexural-torsional buckling load and is always below either P_{ϕ} or P_y^6 . The lower of the two solutions of Equation 2.9 represents the critical buckling load for the member.

The solution of Equation 2.9 in the elastic range is straight forward; the solution of Equation 2.9 in the inelastic range is valid if the section properties used in Equations 2.10 to 2.12 are based on the elastic core remaining at each load interval. The St. Venant torsion resistance is based on the original section⁸. The extent of the remaining elastic core remaining at each load level depends on the residual stress distribution. Residual stresses are induced in a wide flange section by differential cooling and plastic flow after hot rolling. The flange tips cool and stiffen first, then the web cools and must contract against the previously solidified flanges. This cooling sequence results in tensile residual stress in the web and compression stresses at the flange tips. Similar residual stress patterns are formed in angle sections as a result of differential cooling.

Maximum values of residual stresses in rolled wide flange sections have been previously reported. Beedle and Tall¹⁴ report the average value of the peak compressive residual stress as 0.3 of the yield stress for ASTM-A7 steel. Peak values in angle sections have not

been investigated to any extent. However, Galambos⁹ reports the results of two stub column tests on single angles, giving an approximate peak compressive residual stress of 0.30 and 0.22 times the static yield stress. Beedle and Tall³ report a residual stress pattern for angles in riveted columns (Figure 2.3) with a peak value of approximately 0.3 times the yield stress. O'Connor¹⁸ measured residual stresses in random samples of angles (Figure 2.4) in an attempt to establish the residual stress distribution. The stresses reported in these tests did not conform to any consistent pattern.

Test data relating the strength of double angle struts with or without residual stress considerations are almost non-existent. Published work on the buckling strength of other singly symmetric sections in the inelastic range is also meagre.

Galambos⁹ reported the results of tests on single angles loaded axially; the sections deflected in the principal directions with only minor twisting deformations observed. Lenzen¹⁷ has tested open web steel joist sections with double angles used as the top chord members. Tests were performed on single angles and on double angles connected to act as a unit. All failures were associated with flexural buckling or local failure, no torsional failures were reported. Lenzen's results cannot be directly compared to column tests as they represent conditions of loading and end restraint peculiar to joist chord segments.

There is a lack of experimental data on the buckling strength of double angle sections. In addition the buckling strength of such members in the inelastic range has not been determined analytically, and in fact, residual stress distributions for angle sections have not been reported.



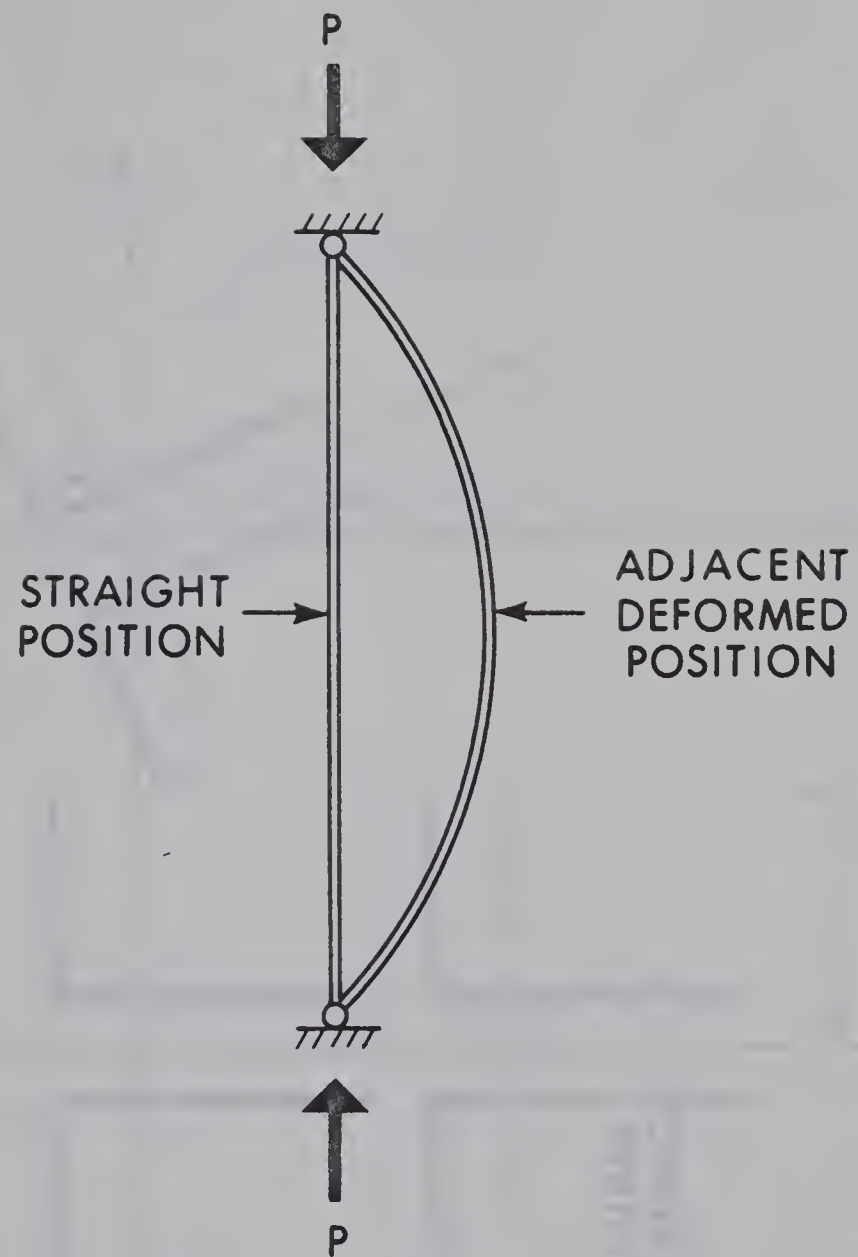


Figure 2.1 Column Equilibrium Positions

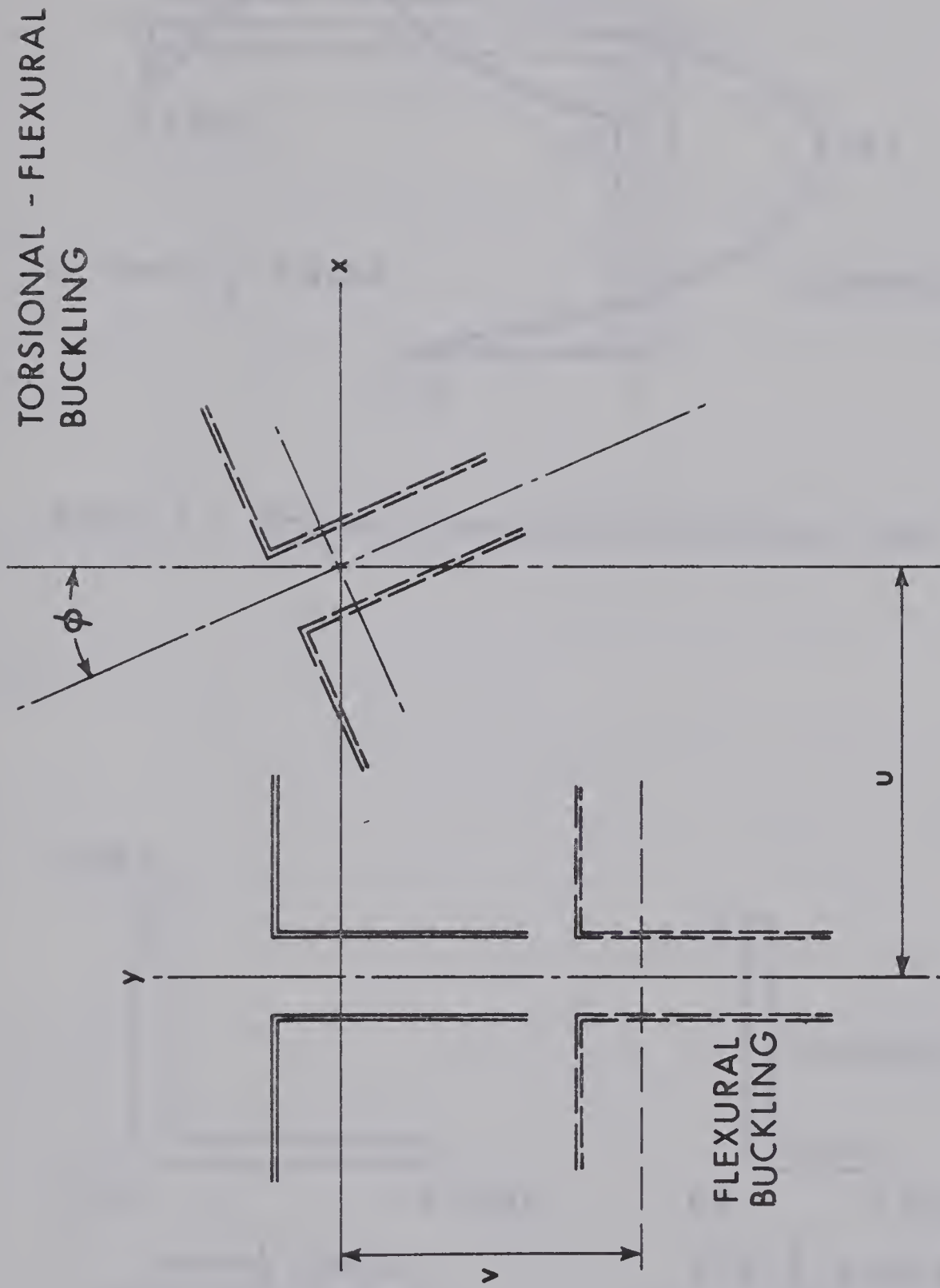


Figure 2.2 Buckling Deformations

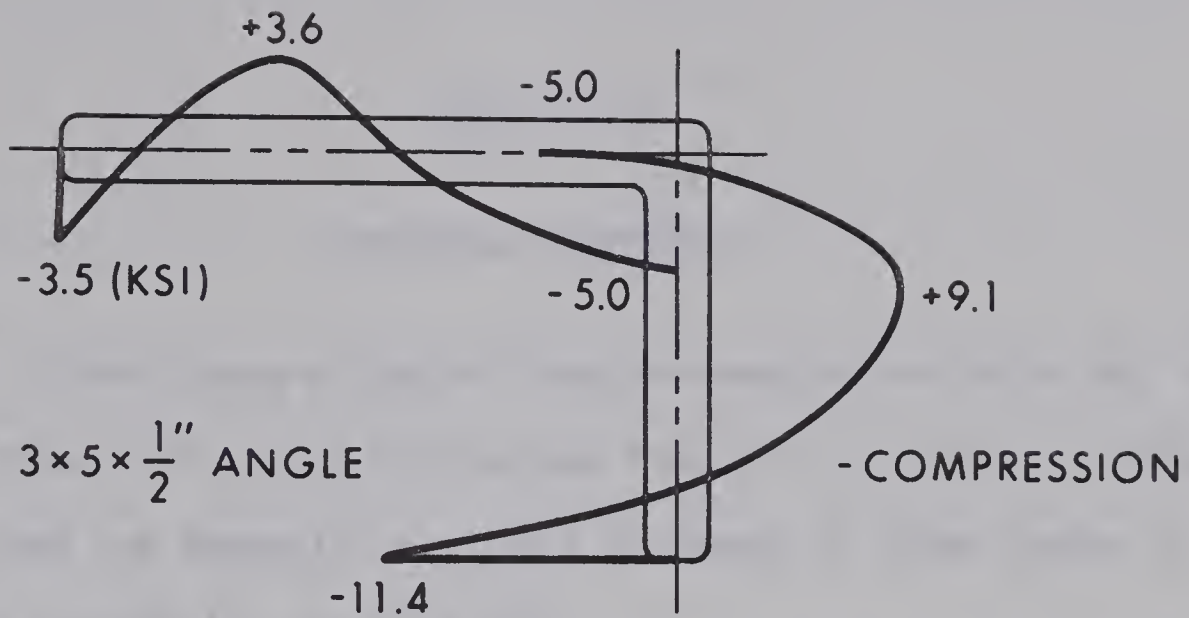


Figure 2.3 Residual Stress-Distribution-Single Angle (Ref. 3)

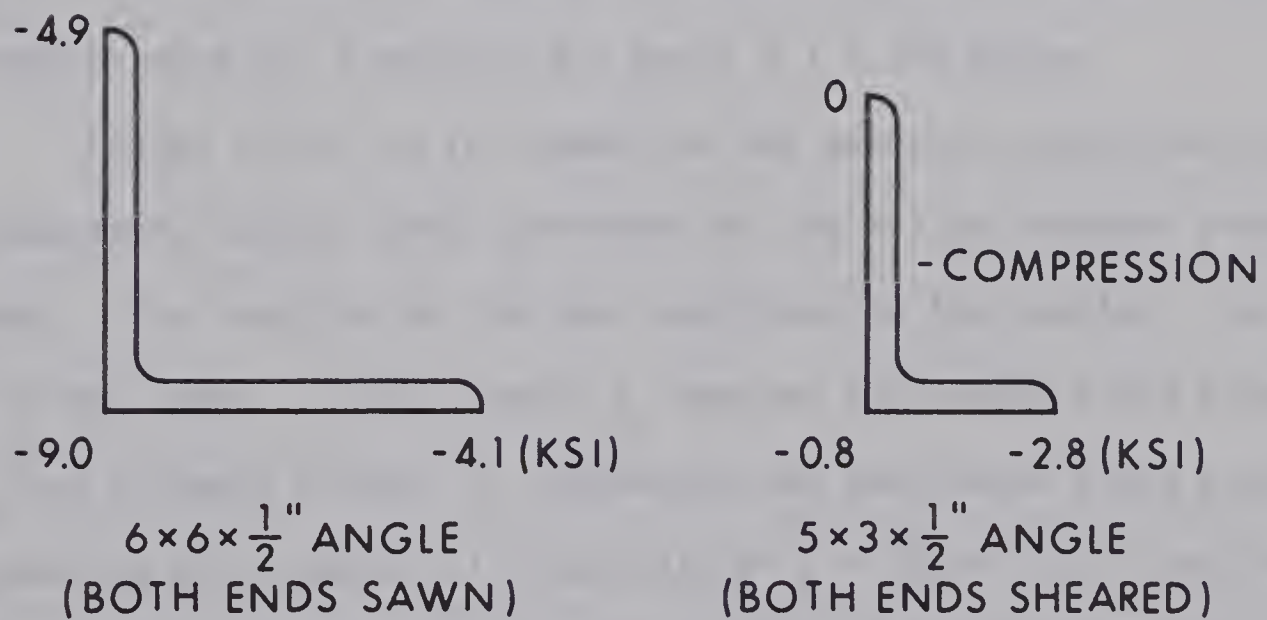


Figure 2.4 Residual Stress Values (Ref. 18)

CHAPTER III

MATERIAL PROPERTIES

A wide range of angle sizes are manufactured with leg lengths varying from 1" to 9" and thicknesses from 1/8" to 1-1/8". The more common sizes are generally available in Canada in three grades of steel; ASTM-A36, CSA-G40.12, and ASTM-A441.

Material properties were obtained from tests on five different angle sections of G40.12 steel. The five sections listed in Table 3.1 were selected to provide a large range of leg lengths and to be large enough to provide easy sectioning.

The chemical composition and mill test results are given in Table 3.1. These results conform to CSA-G40.12 specifications⁷. Mill test results were not available for the 4 x 7 x 3/8 angle.

Tables 3.2(a) to (c) summarize the material properties obtained from laboratory tension tests performed on the milled residual stress specimens. The location of the test specimens in the section are shown in the inset. In this table σ_y denotes the static yield stress and σ_u the ultimate stress; ϵ_y represents the calculated yield strain corresponding to a modulus of elasticity of $E = 29,600 \text{ ksi}$ ¹⁷ and the stress, σ_y . The measured strain at the onset of strain hardening is denoted by ϵ_{st} and E_{st} is the strain hardening modulus. The tests were performed in a Baldwin hydraulic machine using flat tensile specimens

similar in shape to those required by ASTM specification A370-65².

The static yield values were taken after a five minute period at zero strain rate. Values of E_{st} were obtained by graphically measuring the initial slope of the strain-hardening portion of the load-strain curve. The plastic region of the load-strain curve was pronounced in the large majority of the tests with the exception of several specimens from the heel of the angles, which exhibited an elastic-strain hardening response.

Residual stress distributions were obtained by the method of sectioning¹¹. Three test samples were cut from each angle section and the results are plotted individually in Figures 3.1(a) to 3.1(e). Plotted stresses were measured as strains and converted to stresses using $E = 29,600$ ksi. Curvature effects due to bowing upon sectioning were checked²⁰, and found to be negligible. The stress distributions for each angle section were similar with excellent agreement for the three tests performed on a single angle size.

Symmetrical residual stress patterns were not observed even for the equal legged angles. Maximum compressive stresses occurred at or near the heel of the angle in all tests. The maximum compressive residual stress measured was 14 ksi.

The inset in Table 3.3 shows the assumed residual stress patterns used for later computations of the buckling strength. The assumed pattern places maximum compressive residual stress values at the angle heel and leg tips and envelopes the measured values in most

cases. The maximum tensile residual stress is located at the mid point of each leg.

A computer program was developed to ensure that the assumed residual stress distribution did not produce a net axial force or bending moment about the principal axes. The program accepted the residual stresses at the heel and the tip of the short leg as input (σ_{r3} and σ_{r5}) and outputed the remaining peak values.

Table 3.3 lists the values of the measured (average) residual stresses at specific locations and a reasonable balanced computer solution. In Table 3.3 compressive stresses are listed as positive and σ_{r2} is taken at the mid-point of the shorter leg. In addition, the results of a rather extreme balanced case (which represents a maximum compressive residual stress of 13 ksi (as implied in Reference 5) are tabled. Figure 3.2 shows a comparison of the three stress distributions for the 4 x 4 x 3/8" angle.

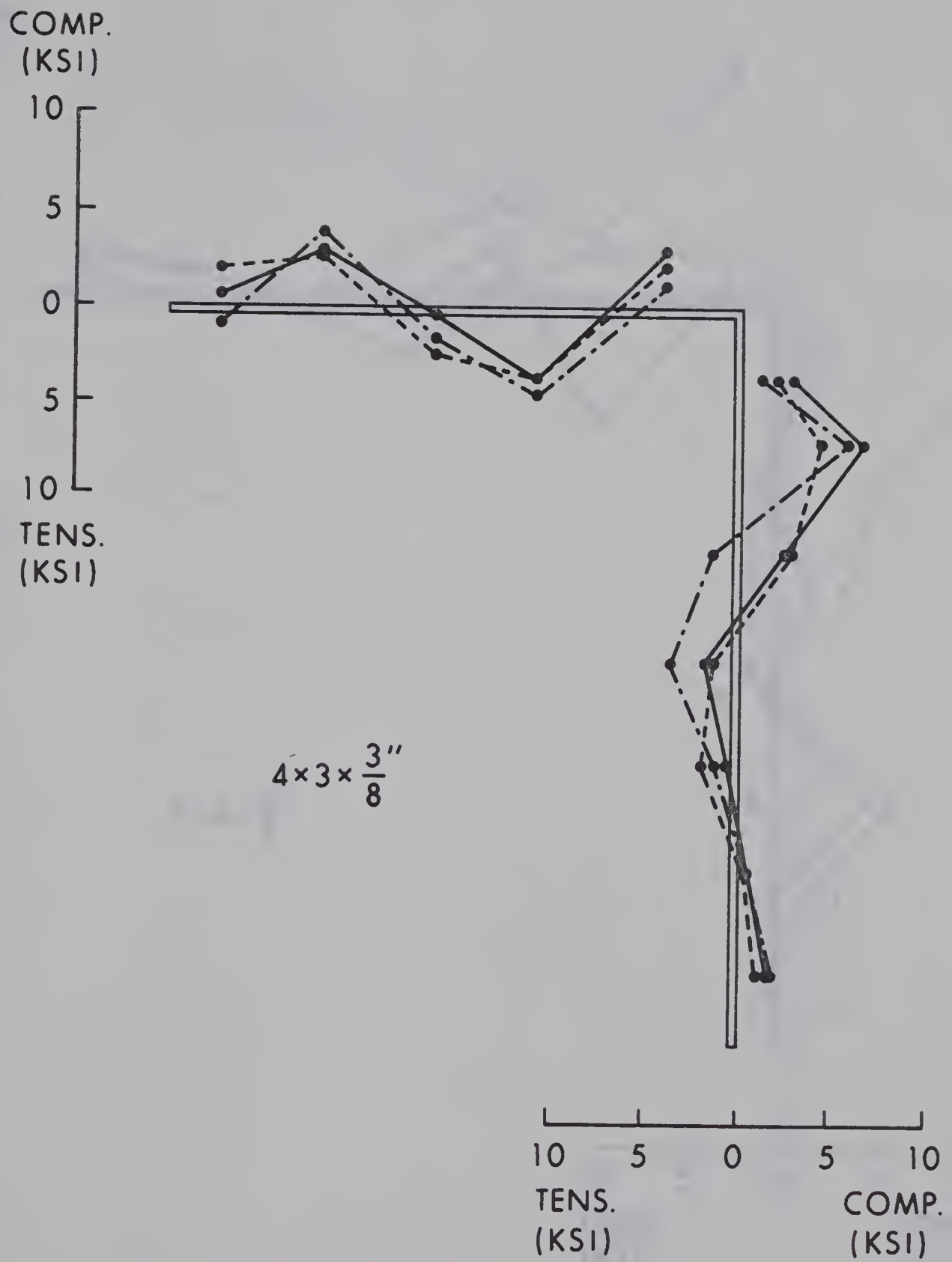


Figure 3.1a Residual Stress Measurements

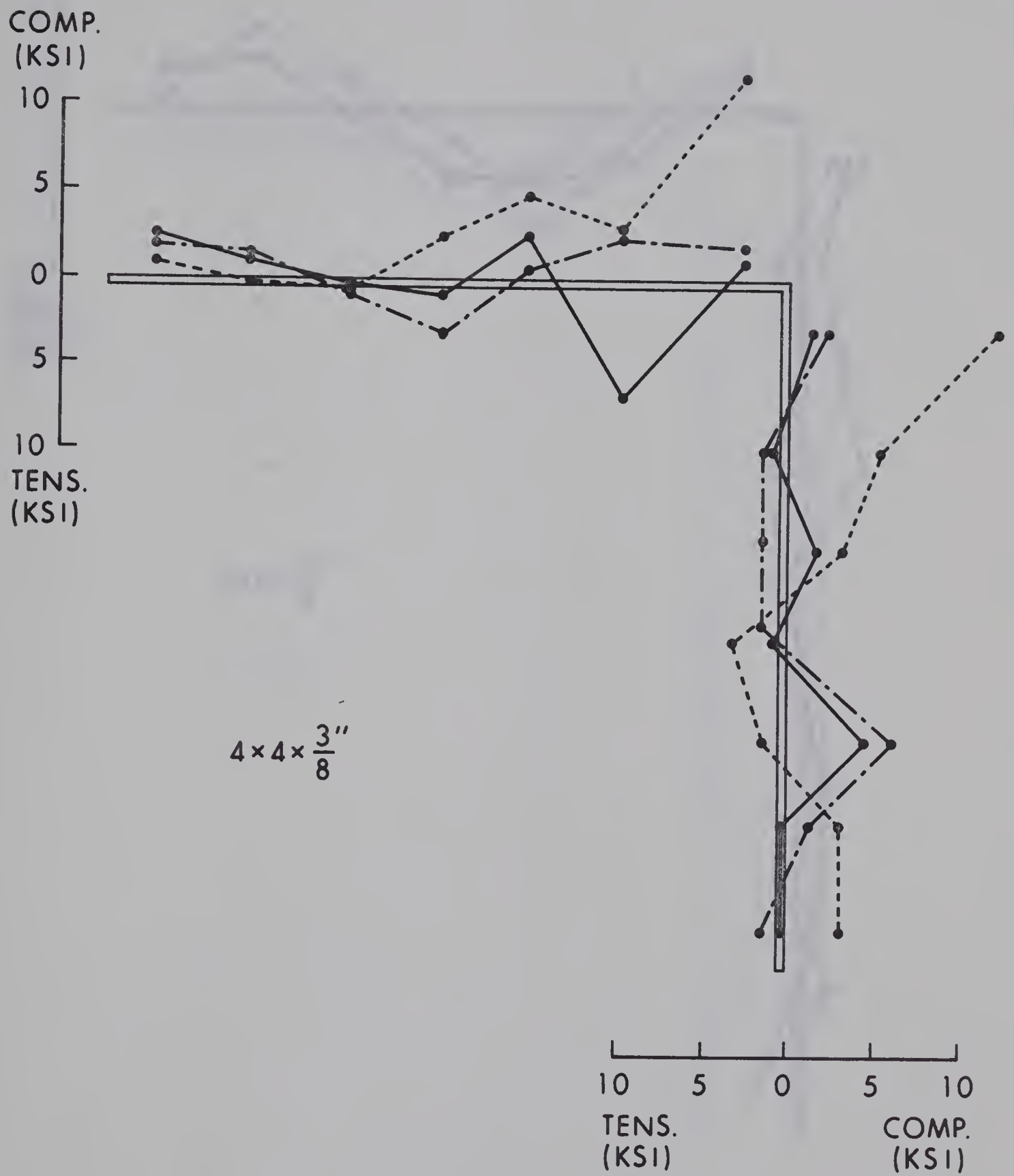


Figure 3.1b Residual Stress Measurements

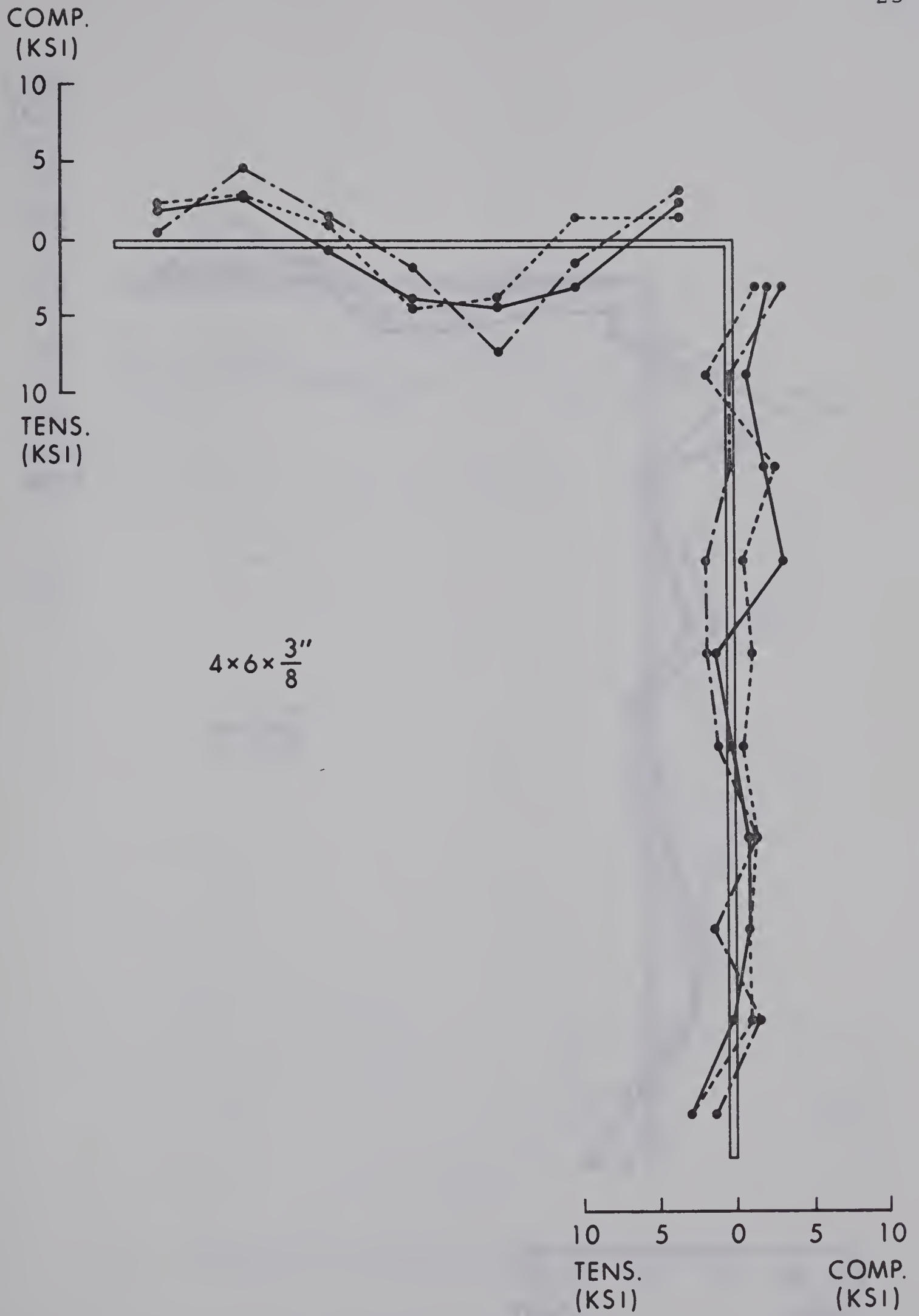


Figure 3.1c Residual Stress Measurements

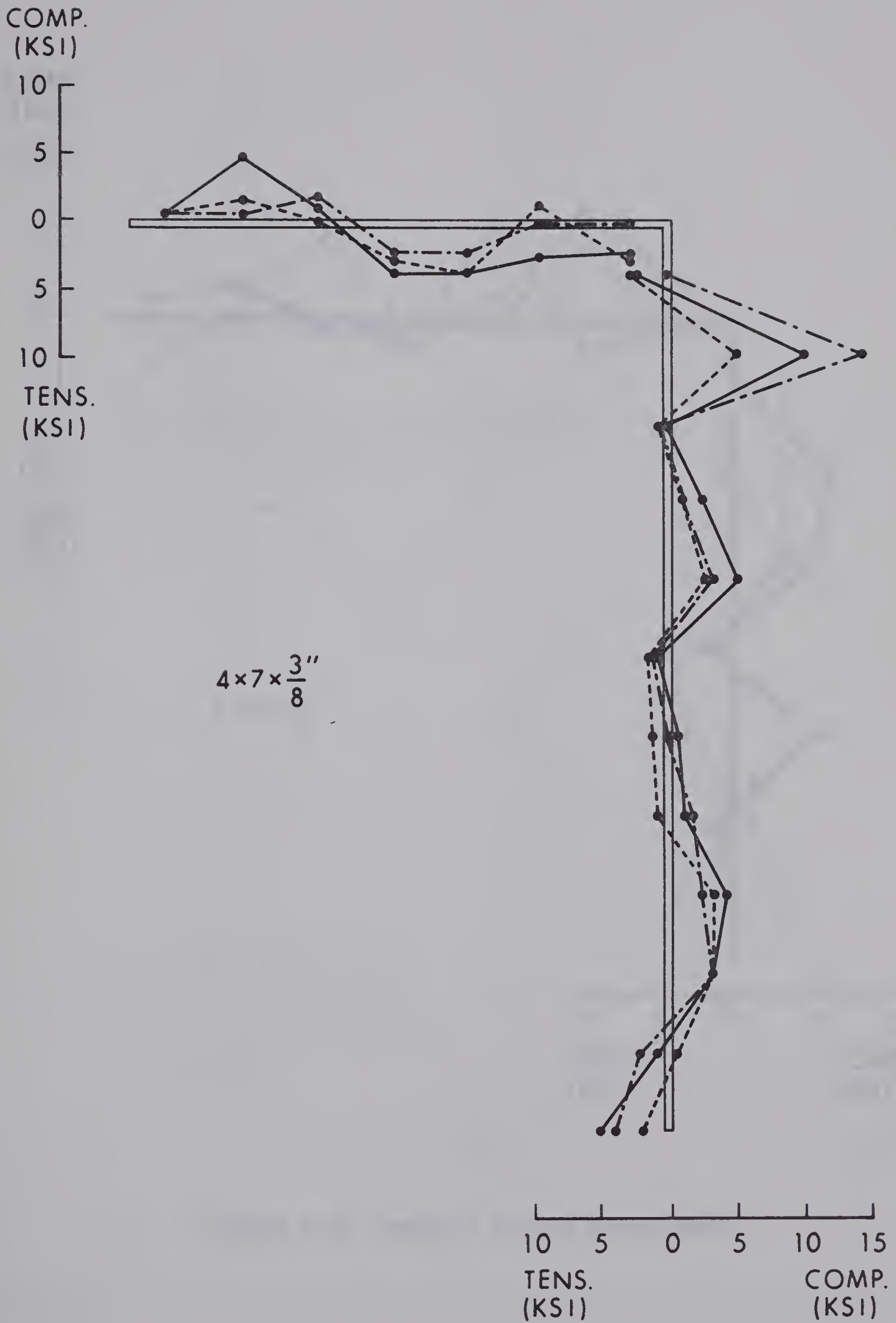


Figure 3.1d Residual Stress Measurements

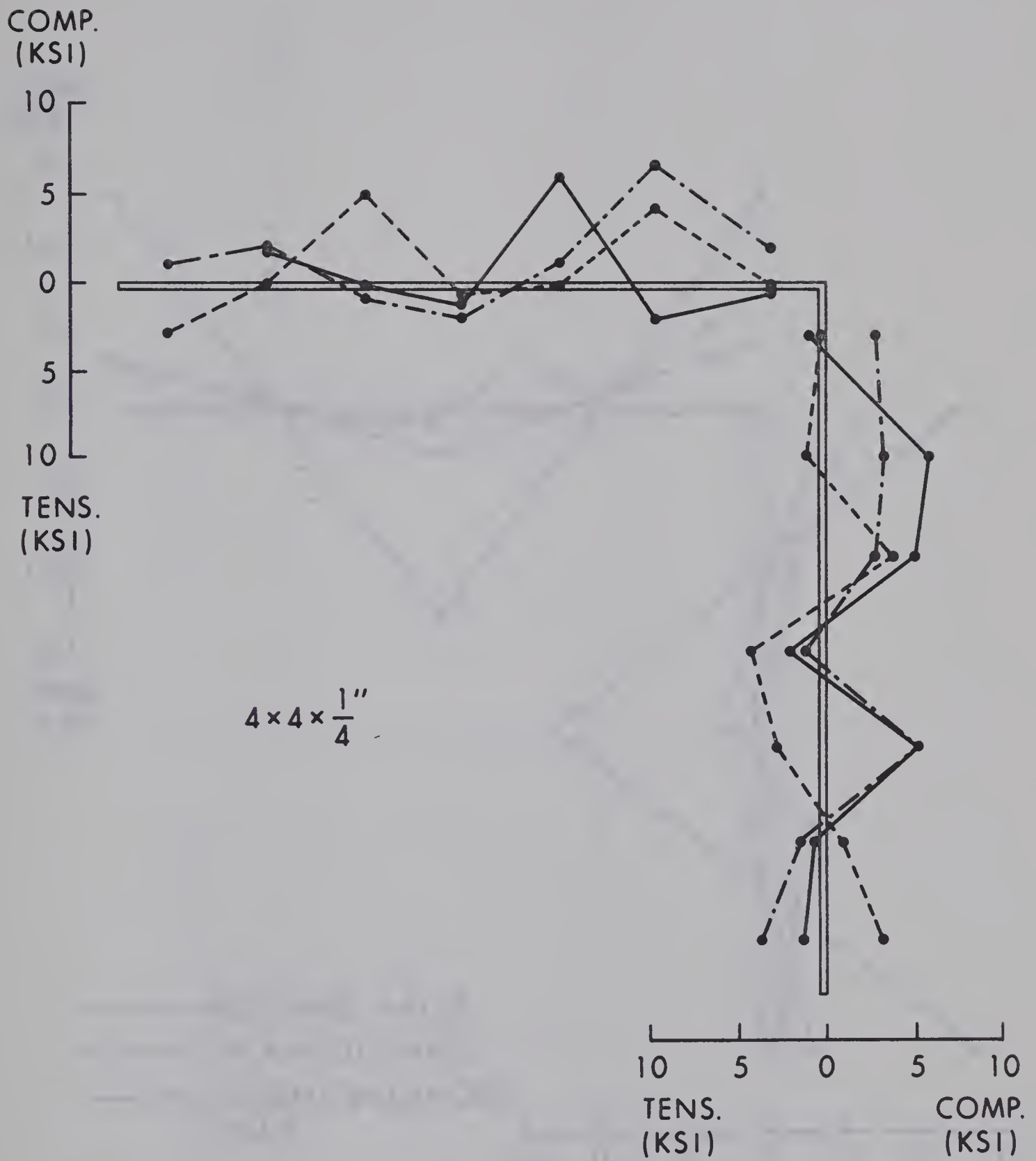


Figure 3.1e Residual Stress Measurements

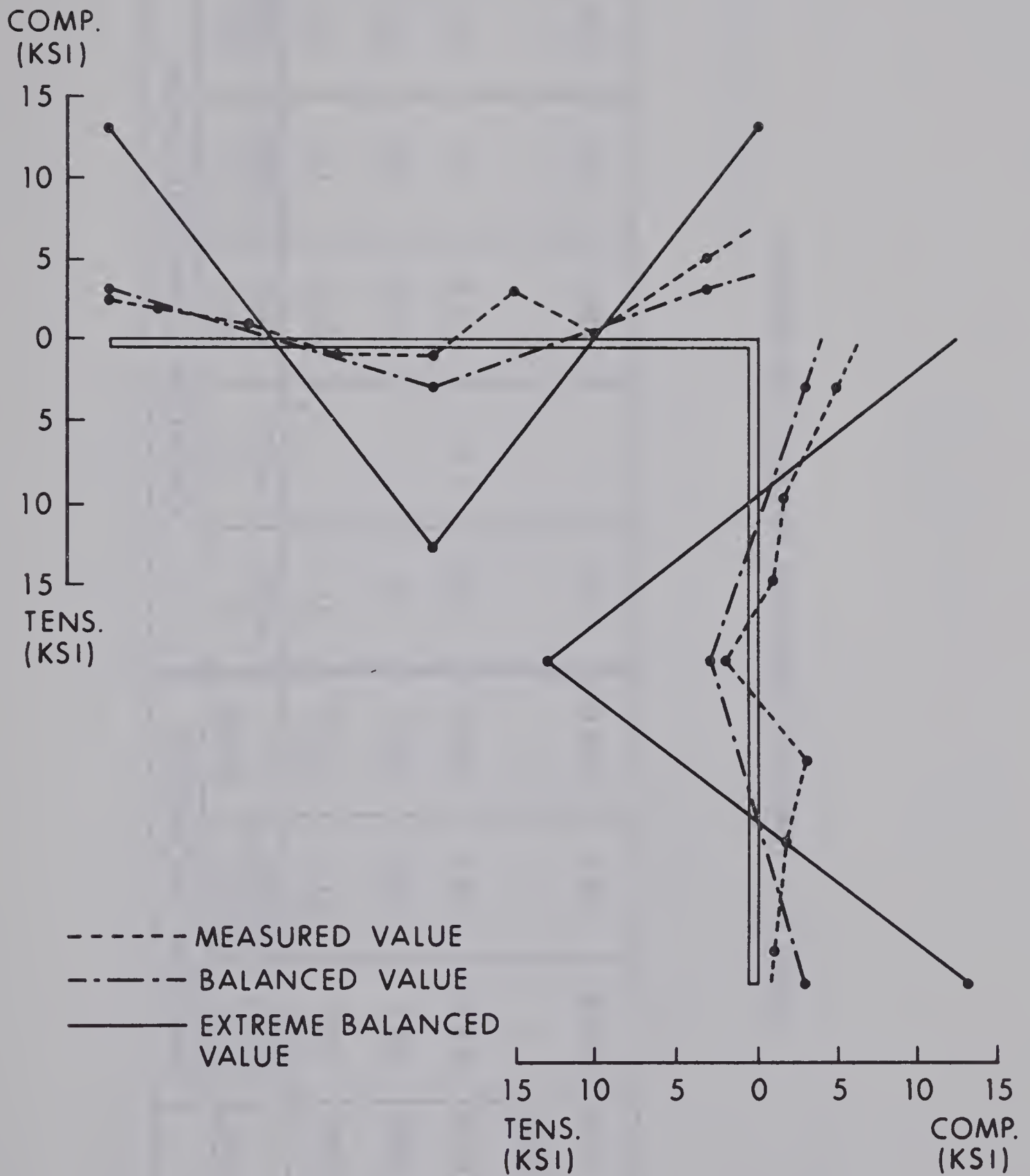


Figure 3.2 Comparison of Residual Stress Distributions (4 x 4 x 3/8") Angle

SECTION	PHYSICAL PROPERTIES			CHEMICAL COMPOSITION %					
	YIELD STRESS (KSI)	ULT. STRENGTH (KSI)	Elong %	C x100	Si x100	Mn x100	P x1000	S x1000	
4x3x3/8	52.2	80.1	20.8	21	-	102	17	32	
4x4x3/8	51.1	76.6	26.7	19	-	102	26	29	
6x4x3/8	47.2	68.1	30.0	20	4	125	9	27	
7x4x3/8	-	-	-	-	-	-	-	-	
4x4x1/4	52.3	76.1	25.0	20	-	92	17	30	

Table 3.1 Chemical Composition and Mill Test Results

ANGLE	SPEC- IMEN	σ_y (KSI)	$\epsilon_y = \frac{\sigma_y}{E^*}$	ϵ_{ST}	E_{ST} (KSI)	σ_u (KSI)	Elong %
4x3x3/8	1	48.2	0.00163	0.0016	796	79.1	29
	2B	47.8	0.00162	0.0068	845	79.9	28
	3	46.4	0.00157	0.0102	909	78.8	29
4x4x3/8	1	44.6	0.00151	0.0117	610	74.5	-
	2A	50.1	0.00169	0.0076	723	79.0	24
	3	46.9	0.00158	0.0076	670	76.8	28
4x6x3/8	1	44.6	0.00151	0.0042	615	73.1	32
	2B	43.8	0.00148	0.0070	657	71.0	33
	3	43.6	0.00147	0.0140	752	70.5	-
4x7x3/8	1	45.2	0.00153	0.0152	567	75.5	32
	2B	59.8	0.00202	0.0202	503	73.7	23
	3	41.8	0.0141	0.0072	352	63.2	-

*NOTE E TAKEN AS 29600 KSI (REFERENCE 17)

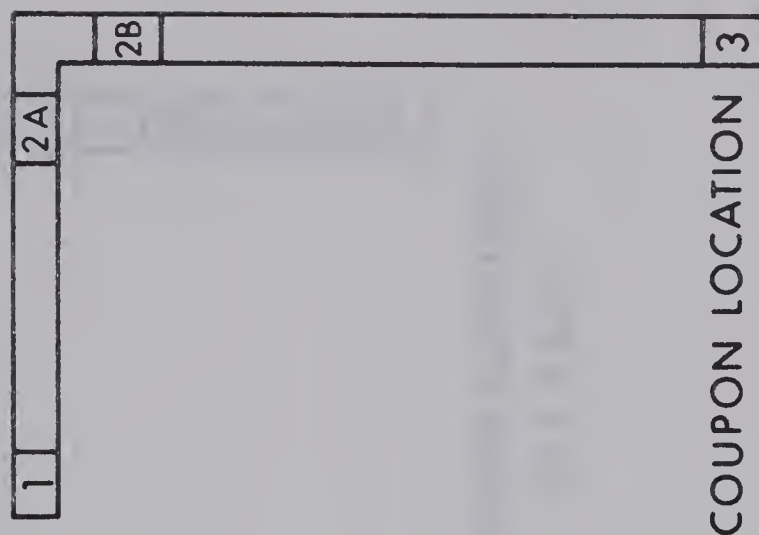
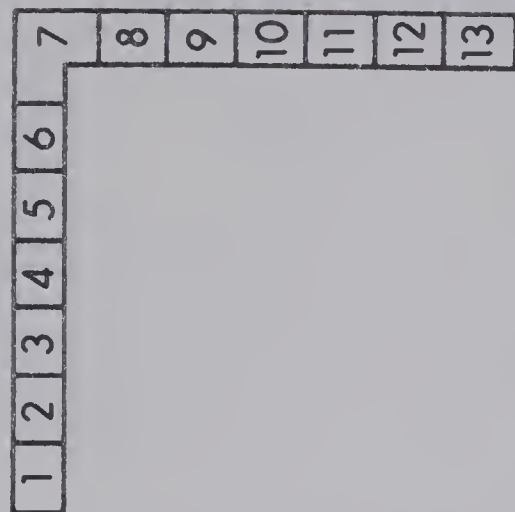


FIGURE 3.2a Material Properties

SPEC- IMEN	σ_y (KSI)	$\epsilon_y = \sigma_y / E^*$	ϵ_{ST}	E_{ST}	σ_u (KSI)	Elong %
1	47.4	0.00160	0.0136	438	75.4	28
2	49.4	0.00167	0.0160	624	80.6	31
3	46.5	0.00157	0.0186	604	76.2	26
4	48.2	0.00163	0.0188	562	77.2	34
5	47.3	0.00160	0.0177	561	76.3	32
6	48.2	0.00163	0.0094	589	78.0	27
7	52.2	0.00177	0.0031	488	78.4	27
8	52.2	0.00177	0.0072	368	79.8	27
9	46.8	0.00158	0.0154	571	76.3	25
10	46.2	0.00156	0.0168	527	76.0	30
11	46.7	0.00158	0.0174	554	76.5	30
12	46.8	0.00158	0.0171	520	76.2	31
13	47.6	0.00161	0.0157	360	76.0	29

*NOTE E TAKEN AS 29600 KSI (REFERENCE 17)



COUPON LOCATION
4 x 4 x 1/4 "

Figure 3.2b Material Properties

SPEC- IMEN	σ_y (KSI)	$\epsilon_y =$ σ_y / E^*	ϵ_{ST}	E_{ST}	σ_u (KSI)	Elong %
1	48.2	0.00163	0.0160	496	75.5	30
2	48.2	0.00163	0.0190	577	78.0	28
3	48.3	0.00163	0.0180	362	78.5	30
4	47.9	0.00162	0.0196	495	77.5	30
5	46.7	0.00158	0.0147	452	78.8	31
6	47.3	0.00160	0.0178	480	77.6	29
7	47.2	0.00160	0.0045	678	78.4	27
8	47.1	0.00159	0.0132	582	76.2	27
9	48.3	0.00163	0.0182	670	78.6	28
10	49.3	0.00167	0.0166	894	77.6	30
11	48.6	0.00165	0.0202	448	78.3	31
12	49.2	0.00166	0.0162	470	78.0	-
13	50.9	0.00172	0.0168	464	78.0	28

*NOTE E TAKEN AS 29600 KSI (REFERENCE 17)

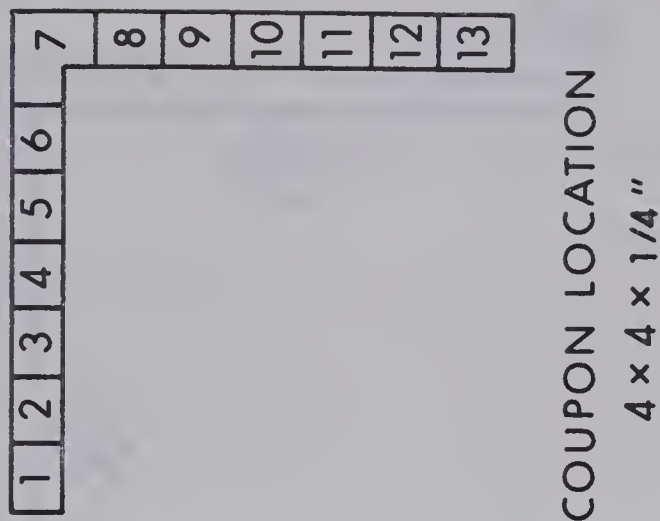
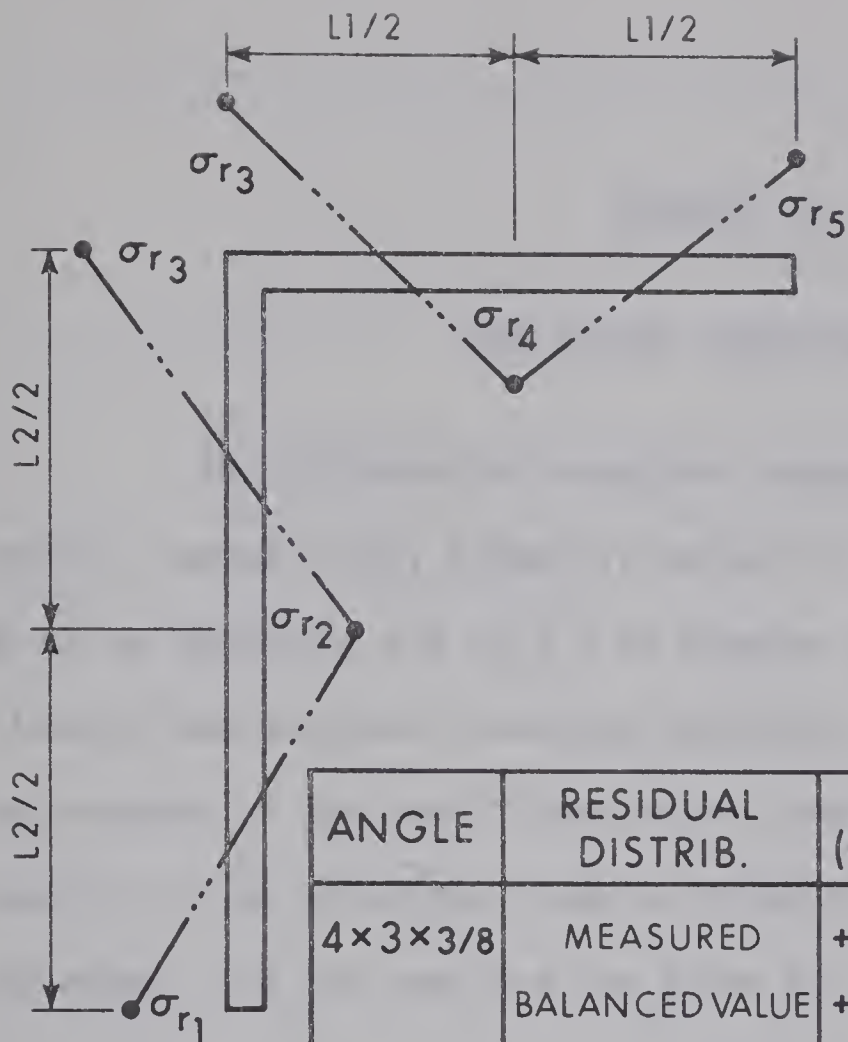


Figure 3.2c Material Properties



ANGLE	RESIDUAL DISTRIB.	σ_{r1} (KSI)	σ_{r2} (KSI)	σ_{r3} (KSI)	σ_{r4} (KSI)	σ_{r5} (KSI)
4×3×3/8	MEASURED	+ 2.0	- 3.0	+ 5.0	- 5.0	+ 1.0
	BALANCED VALUE	+ 5.7	- 5.6	+ 5.0	- 4.2	+ 4.0
	EXTREME BAL- ANCED VALUE	+13.0	-13.0	+13.0	-13.0	+13.0
4×4×3/8	MEASURED	+ 2.0	- 1.0	+ 5.0	- 2.0	+ 1.0
	BALANCED VALUE	+ 3.0	- 3.0	+ 3.0	- 3.0	+ 3.0
	EXTREME BAL- ANCED VALUE	+13.0	-13.0	+13.0	-13.0	+13.0
4×6×3/8	MEASURED	+ 2.0	- 5.0	+ 2.0	- 1.0	+ 1.0
	BALANCED VALUE	+2.3	-2.4	+ 3.0	-3.8	+4.0
	EXTREME BAL- ANCED VALUE	+13.0	-13.0	+13.0	-13.0	+13.0
4×7×3/8	MEASURED	+ 0.0	- 4.0	+10.0	- 1.0	+ 4.0
	BALANCED VALUE	+ 7.1	-6.9	+ 6.0	-4.3	+ 4.0
	EXTREME BAL- ANCED VALUE	+13.0	-13.0	+13.0	-13.0	+13.0
4×4×1/4	MEASURED	- 2.0	- 3.0	+ 6.0	- 3.0	+ 3.0
	BALANCED VALUE	+ 3.0	- 3.0	+ 3.0	- 3.0	+ 3.0
	EXTREME BAL- ANCED VALUE	+13.0	-13.0	+13.0	-13.0	+13.0

* COMPRESSION POSITIVE (+)

TABLE 3.3 Residual Stress Distribution Values

CHAPTER IV

ANALYTICAL INVESTIGATION

The differential equations expressing equilibrium of an axially loaded singly symmetric column in the deformed position were given as equations 2.6 to 2.8 in Chapter II. For simply supported flexural and torsional boundary conditions, the condition that the determinant of the coefficient matrix vanishes (buckling condition) results in the solutions given by equation 2.9. Of the three possible solutions, two are real and are given by:

$$P_x = \frac{\pi^2 EI_x}{L^2} \quad (4.1)$$

and $P_{\phi y}$ equal to the root of:

$$-\frac{K}{P} (P - P_y)(P - P_\phi) - P_{y_0}^2 \quad (4.2)$$

The evaluation of equations 4.1 and 4.2 requires known values of the section properties and the column length, to calculate the two critical buckling loads, P_x and $P_{\phi y}$. In the elastic range the critical loads corresponding to a given length can be determined directly, but in the inelastic range the section properties depend on the extent of yielding across the section, which in turn is influenced by the applied

load. Thus an indirect approach must be used to solve Equations 4.1 and 4.2.

An elastic-plastic stress-strain curve (Figure 4.1) is assumed for the material. The cross-section is divided into segments and a uniform strain, ϵ_a , is applied to the entire cross-section. The total strain in any segment, ϵ_t , is then equal to the sum of the applied strain, ϵ_a , and the residual strain, ϵ_r .

$$\epsilon_t = \epsilon_a + \epsilon_r \quad (4.3)$$

The stress-strain curve can be entered with the total strain and the corresponding stress in the segment, σ , is determined as shown in Figure 4.1. The total load, P , on the cross-section corresponding to the applied strain level and the assumed residual strain pattern can be calculated as:

$$P = \int_A \sigma dA \quad (4.4)$$

The factor \bar{K} which arises from the differential warping of two adjacent cross-sections can be calculated as:

$$\bar{K} = \int_A \sigma a^2 dA \quad (4.5)$$

where a represents the distance of the segment under consideration

from the shear centre.

At a zero applied strain level the value of \bar{K} represents the reduction in torsional buckling strength due to the residual strain distribution. This reduction is applicable in both the elastic and inelastic ranges.

The flexural and torsional section properties are calculated by assuming that no resistance is offered by the yielded segments. All section property calculations are based on thin wall theory⁸. The calculation of the St. Venant torsional resistance, K_T , is performed on the original elastic cross-section⁸. For a given level of applied strain, ϵ_t , the corresponding applied load and section properties are then known. Equation 4.1 and 4.2 can then be solved directly to obtain the lengths corresponding to flexural and lateral-torsional buckling, L_x and $L_{\phi y}$, respectively.

A computer program listed in Appendix A, was developed to calculate the flexural and torsional section properties and solve the buckling equations at various applied strain levels. A simplified flow chart for the computer program is given in Figure 4.4.

The warping moment of inertia, I_w , was computed by assuming that the two angles were joined on the gauge line by a thin strip, as shown in Figure 4.3. The value of I_w for a single angle is zero⁹ thus the angle sections must act as a unit for the warping moment of inertia to have a finite value.

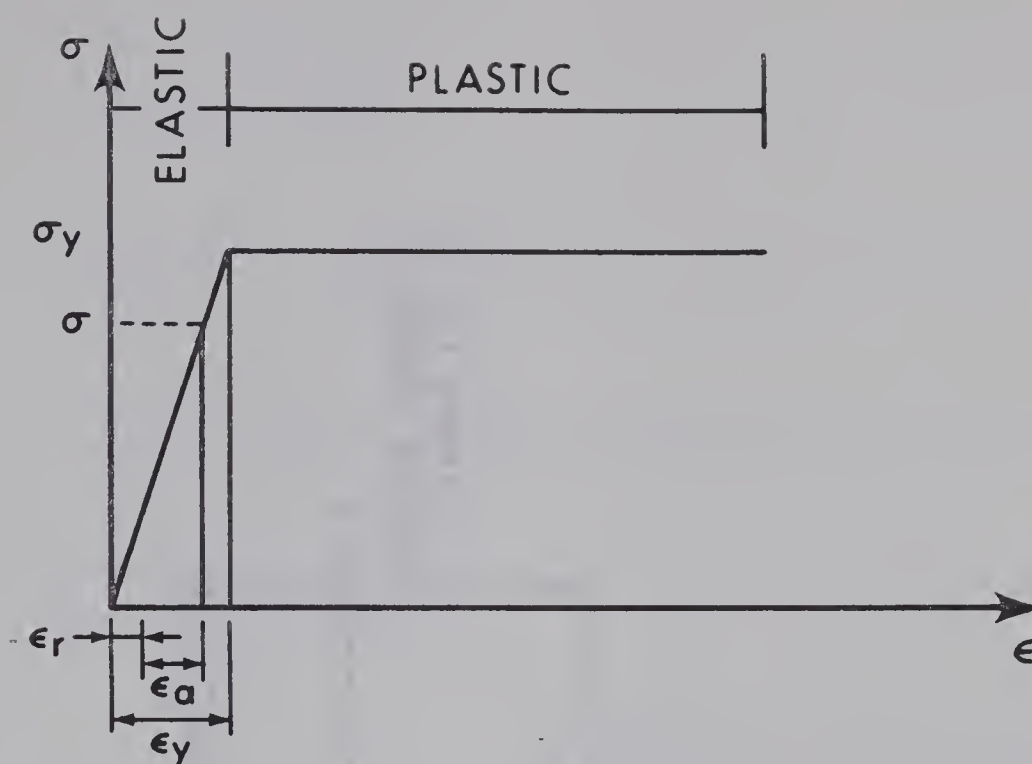
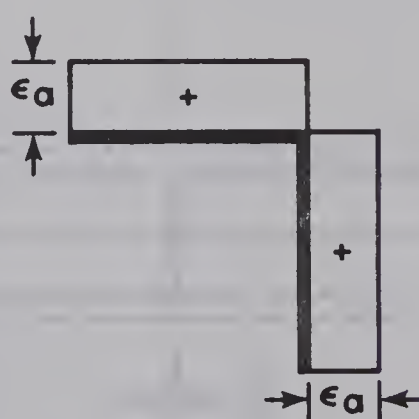
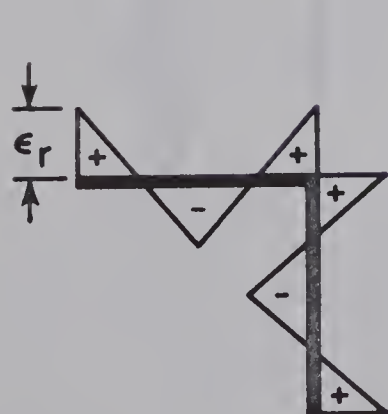


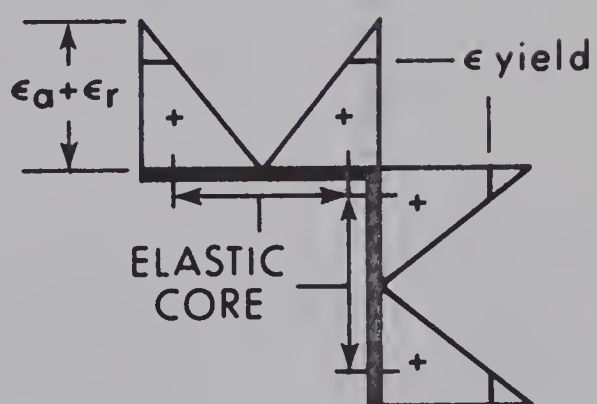
Figure 4.1 Stress-Strain Curve



UNIFORM APPLIED STRAIN
(+ COMPRESSIVE STRAIN)



RESIDUAL STRAIN PATTERN



TOTAL STRAIN

Figure 4.2 Strain Patterns

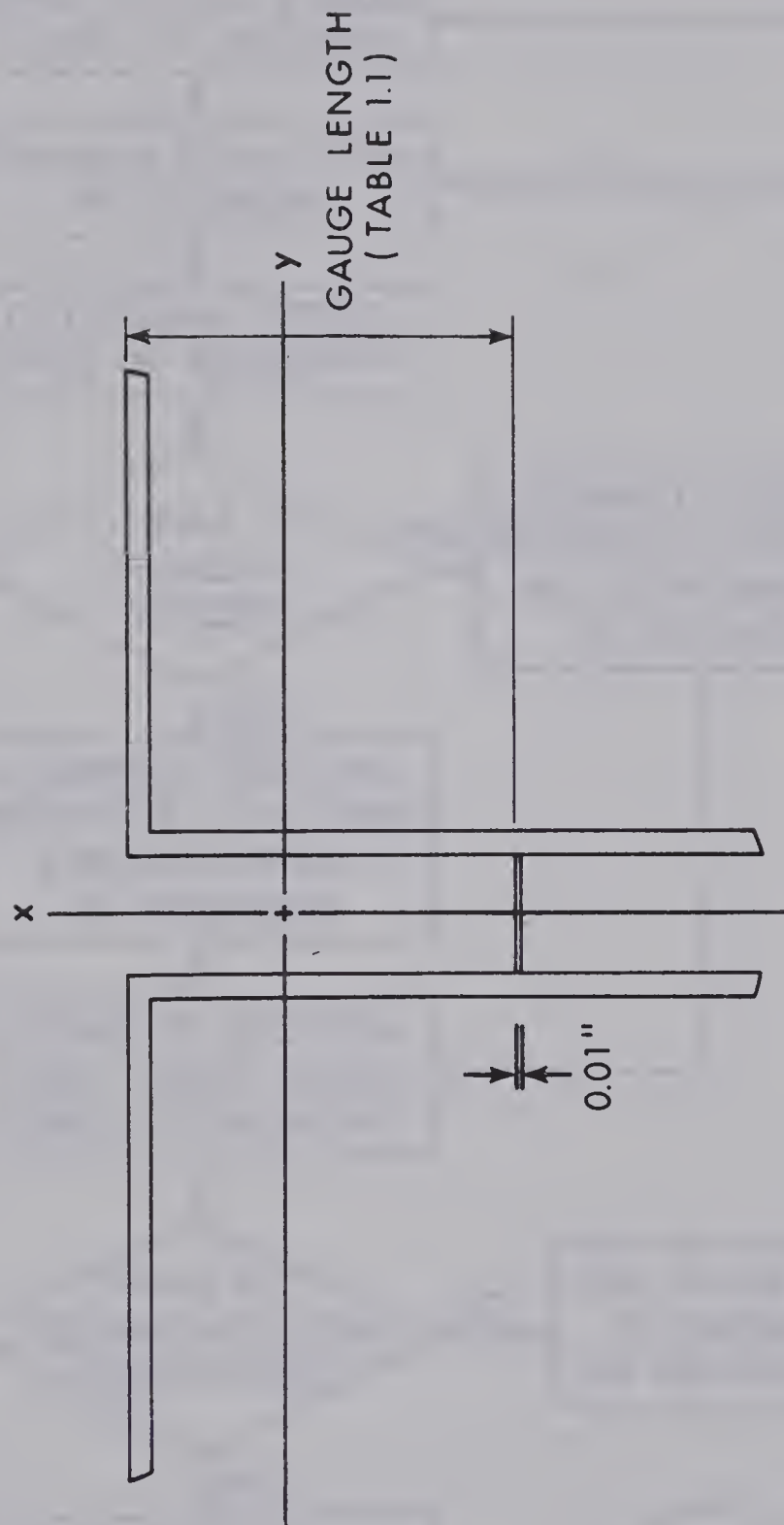


Figure 4.3 Double Angle Connection at Gauge Location

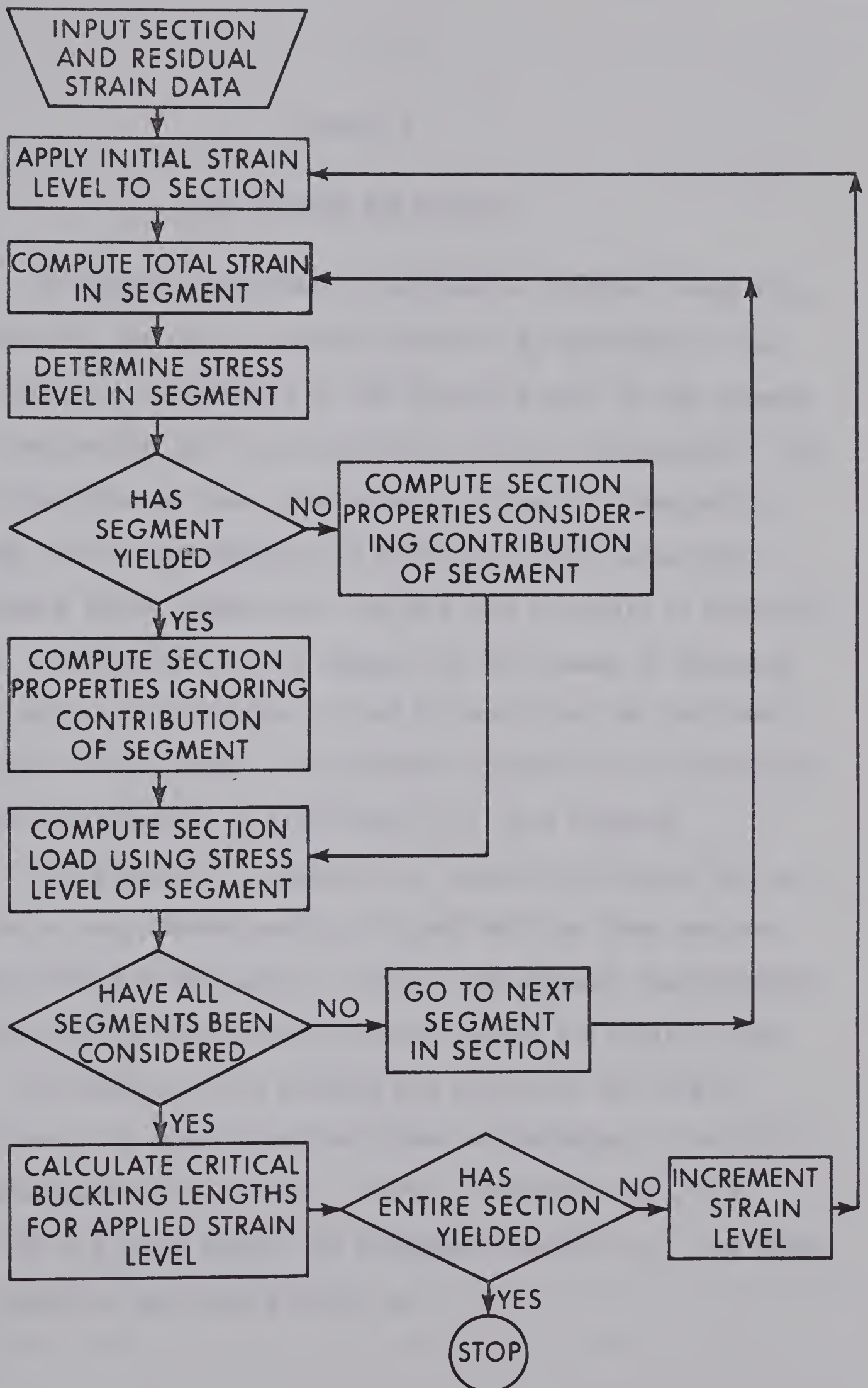


Figure 4.4 Flow Chart for Computer Program

CHAPTER V

TEST PROGRAM AND RESULTS

The analysis described in the previous chapters proceeds by first selecting the level of applied strain to be considered. The applied strain is superimposed on the residual strain in each segment of the cross-section and the corresponding stress is determined. The section properties are then computed using a numerical integration procedure; the yielded segments are omitted from this calculation. Approximately eighty segments per leg were used to obtain an accurate solution. The stresses on each segment are then summed to determine the applied load and Equations 4.1 and 4.2 are solved for the corresponding equilibrium lengths. In addition, Equation 2.10 is solved for the length corresponding to (fictitious) y-y axis buckling.

This procedure is repeated for increasing values of the applied strain level, corresponding to higher buckling loads and progressive yielding of the member. Finally, the complete cross-section has yielded and the corresponding buckled lengths are equal to zero.

The results of the analyses are plotted in the form of column curves. In these curves the stress corresponding to buckling, σ , is non-dimensionalized as σ/σ_y , where σ_y represents the yield stress, and is plotted against the slenderness ratio, L/r_x . The value of σ is given, at each strain level, by:

$$\sigma = \Sigma \frac{\bar{\sigma} \Delta A}{A} \quad (5.1)$$

where $\bar{\sigma}$ represents the stress on a particular segment of the cross-section and ΔA represents the area of the segment.

The results are presented in Figures 5.1 to 5.5. In each case two curves are given; that corresponding to x-x axis flexural buckling and that corresponding to lateral-torsional buckling. Each curve has two portions; the elastic (concave) portion pertaining to large values of L/r_x and the inelastic (convex) portion for smaller slenderness ratios. In general, the curves corresponding to flexural buckling are shown as dashed and those corresponding to lateral-torsional buckling as solid curves.

The curves corresponding to (fictitious) y-y axis buckling are not shown. In all cases, however, they lie just above the curves corresponding to lateral-torsional buckling. For a given slenderness ratio, the critical stresses are within 2% of one another. Those shown in Table 5.1 coincide in the second decimal place.

Influence of Angle Symmetry - Figures 5.1(a) through 5.1(e) show column curves for five double angle sections. The sections are composed of angles ranging from the $3\frac{1}{2} \times 2\frac{1}{2} \times \frac{5}{16}$ " to a $7 \times 4 \times \frac{3}{8}$ ". In addition to variations in size the angles have differing ratios of r_x to r_y ; where r_x denotes the radius of gyration of the section about the x axis and r_y the radius of gyration about the y axis. For example, the $7 \times 4 \times \frac{3}{8}$ " angle has a ratio of 1.43 while the $4 \times 4 \times \frac{3}{8}$ " has a ratio of 0.66. Each of the curves shown in Figure 5.1 was obtained for a member having a

yield stress level of 44 ksi, a maximum compressive residual stress of 13 ksi and the section is formed by placing the long legs of the angles back to back. The separation, assumed to be caused by a gusset plate, was related to the leg thickness. In the analysis, the angles were assumed to act as a unit, connected at the gauge line (Table 1.1).

The members having large values of r_y (r_x/r_y ratios ≤ 1.0) have lateral-torsional buckling strengths greater than flexural buckling strengths. As r_x/r_y increases above unity the trend reverses. This is shown for example, by a comparison of the curves for the $4 \times 4 \times \frac{3}{8}$ " ($r_x/r_y = 0.66$) angle (Figure 5.1(c)) with curves for the $7 \times 4 \times \frac{3}{8}$ " ($r_x/r_y = 1.43$) angle (Figure 5.1(e)). This is as expected since the lateral-torsional buckling loads and the y-y flexural buckling loads are virtually coincident. Note that in some cases cross-overs occur in the inelastic range (for example see Figure 5.1(a)).

Influence of Leg Thickness - Figures 5.2(a) through 5.2(e) show column curves for double angle sections. The sections are composed of 6" x 4" angles ranging in thickness from 5/16" to 3/4". The radius of gyration ratios fall within a relatively narrow range, from 1.20 for the 5/16" leg thickness to 1.05 for the 3/4" thick angle section. The angles are placed with the long legs back to back and the assumed gusset plate thickness is compatible with the leg thickness of the angles. The members analyzed had a yield stress of 44 ksi and a maximum compressive residual stress of 13 ksi.

The members all have small values of r_y (r_x/r_y ratios > 1.0)

which produces flexural buckling strengths greater than lateral-torsional buckling strengths. Note that in some cases cross-overs do occur in the inelastic range (Figure 5.2(d)).

Influence of Angle Separation - Figure 5.3 shows the column curves for double angle sections composed of $6 \times 4 \times \frac{3}{8}$ " angles having the long legs back to back. The gusset plate thickness (separation of the long legs) ranges from $\frac{3}{8}$ " to $\frac{3}{4}$ ". The radius of gyration ratios range from 1.19 for the $\frac{3}{8}$ " separation to 1.10 for the $\frac{3}{4}$ " separation. The yield stress level and residual stress distribution were the same as the previous analyses. The flexural buckling curves for the four members coincide. The lateral-torsional strengths vary, however, as shown by the solid curves.

The members again illustrate dominant flexural buckling strengths with lateral-torsional buckling strengths approaching the flexural strengths as the ratio r_x/r_y approaches unity.

Influence of Yield Stress Level - Figures 5.4(a) through 5.4(d) show column curves for double angle sections composed of $6 \times 4 \times \frac{3}{8}$ " angles having the long legs back to back, and a constant gusset plate thickness of $\frac{5}{8}$ ". The yield stress levels were varied to represent four common materials; 36 ksi yield-ASTM-A36, 44 ksi yield-CSA-G40.12, 50 ksi yield-ASTM-A441 and 100 ksi yield-ASTM-A514. The maximum compressive residual stress was assumed to be 13 ksi for all members.

The flexural buckling strengths were greater than the lateral-torsional strengths in all cases as the ratio r_x/r_y was

greater than unity. An increase in the yield stress level effectively increases the elastic limit, since the ratio of maximum compressive residual stress to yield stress is reduced. For example ASTM-A36 steel has an elastic limit of $0.64 \sigma_y$ corresponding to a slenderness ratio of approximately 100 for lateral-torsional buckling, whereas ASTM-A514 has an elastic limit of $0.87 \sigma_y$ corresponding to a slenderness ratio of approximately 50.

Influence of Residual Stress Distribution - Figure 5.5 shows the column curves for double angle sections composed of $7 \times 4 \times \frac{3}{8}$ " angles having the long legs back to back and a constant gusset plate thickness of $\frac{5}{8}$ ". The yield stress level was held constant at 44 ksi, with three different residual stress distributions. The $7 \times 4 \times \frac{3}{8}$ " angle was used as this represented the section with the maximum measured residual stress (14 ksi compressive). The first distribution corresponded to the unbalanced measured values; these were then balanced by a computer solution (Chapter IV) for the second distribution. The third balanced distribution was based on the recommendations of CSA-S16 and has a maximum compressive residual stress of 13 ksi.

The flexural buckling strengths were greater than lateral-torsional buckling strengths for these members, as the ratio of r_x/r_y exceeded unity. The unbalanced measured residual stress distribution produced the maximum buckling strengths for both buckling modes, although the curves showed a sudden break when a substantial portion of the cross-section had yielded. The balanced measured distribution smoothed out

the column curves and the ultimate strengths were below those obtained with the unbalanced distribution. The 13 ksi maximum compressive residual stress distribution was below the other corresponding curves and produced a conservative estimate of the buckling strengths.



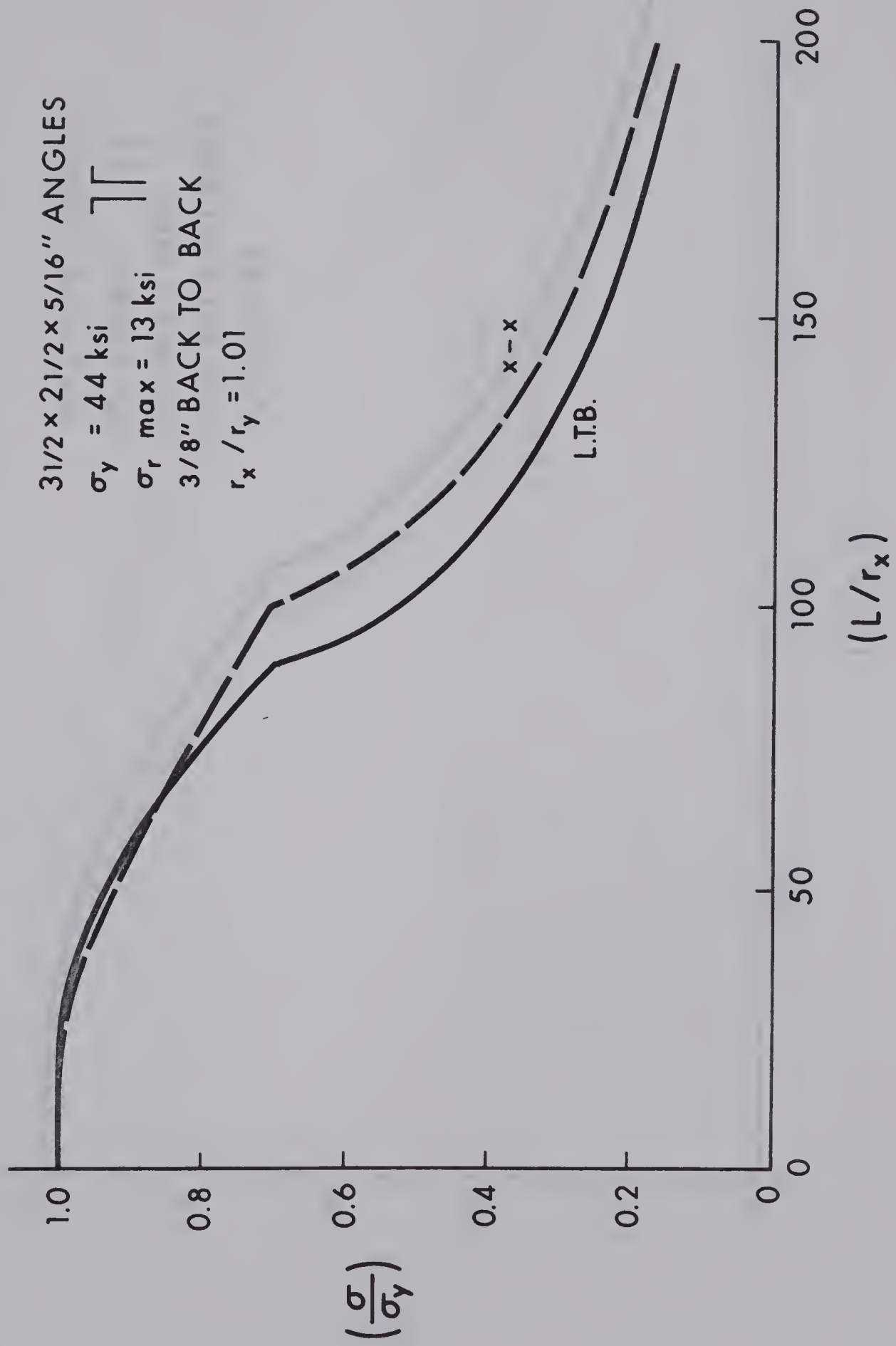


Figure 5.1a Influence of Member Asymmetry

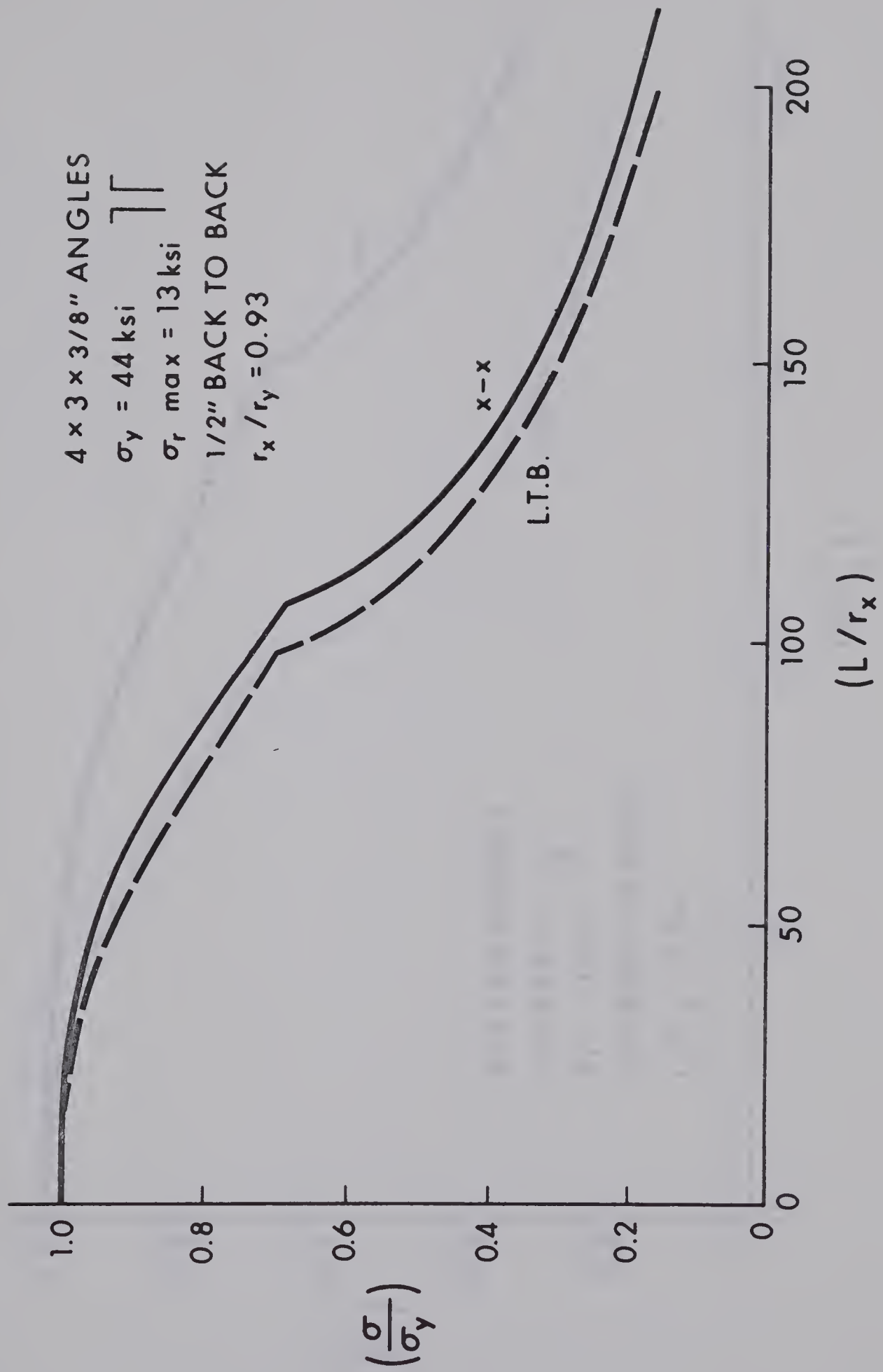


Figure 5.1b Influence of Member Asymmetry

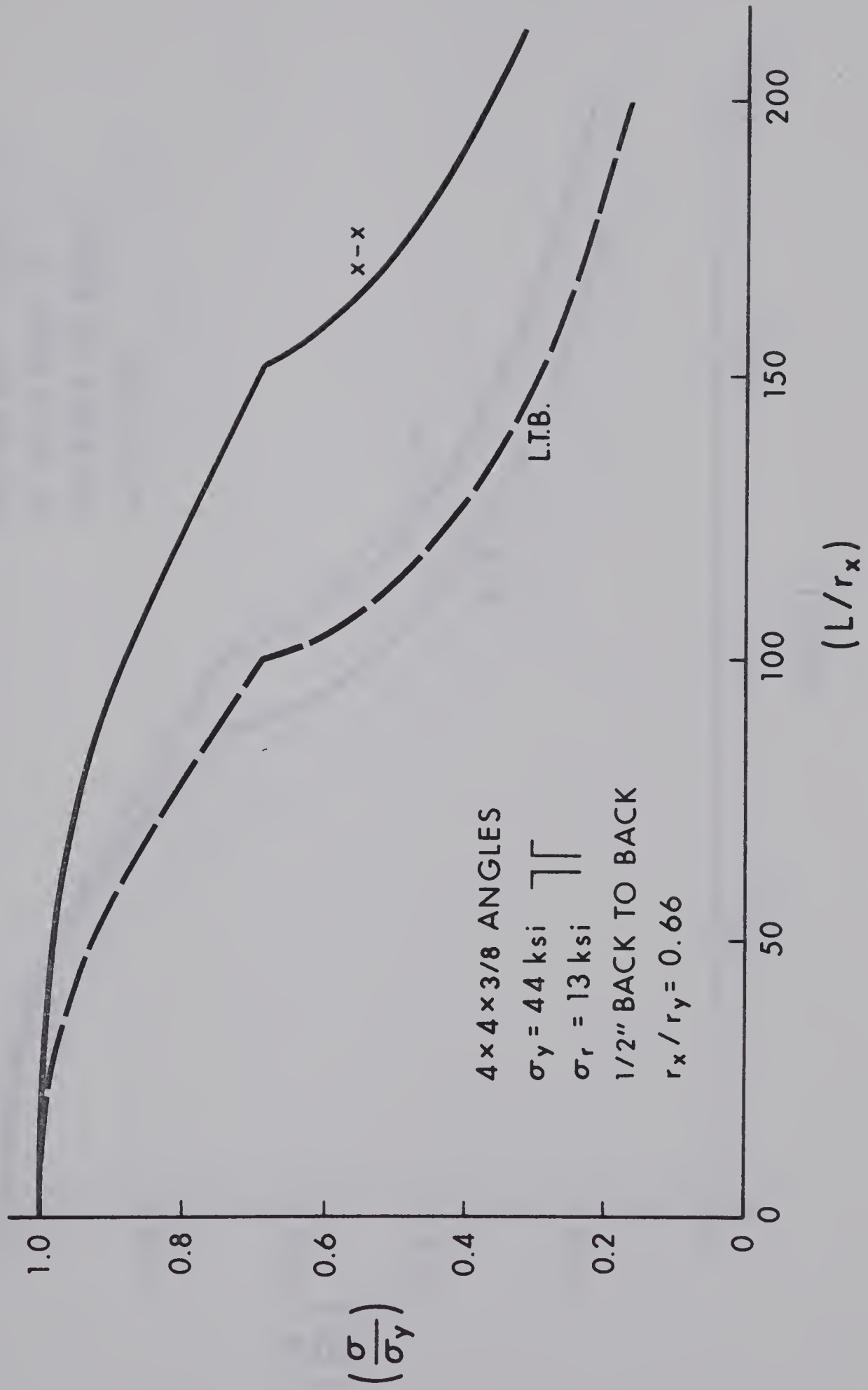


Figure 5.1c Influence of Member Asymmetry

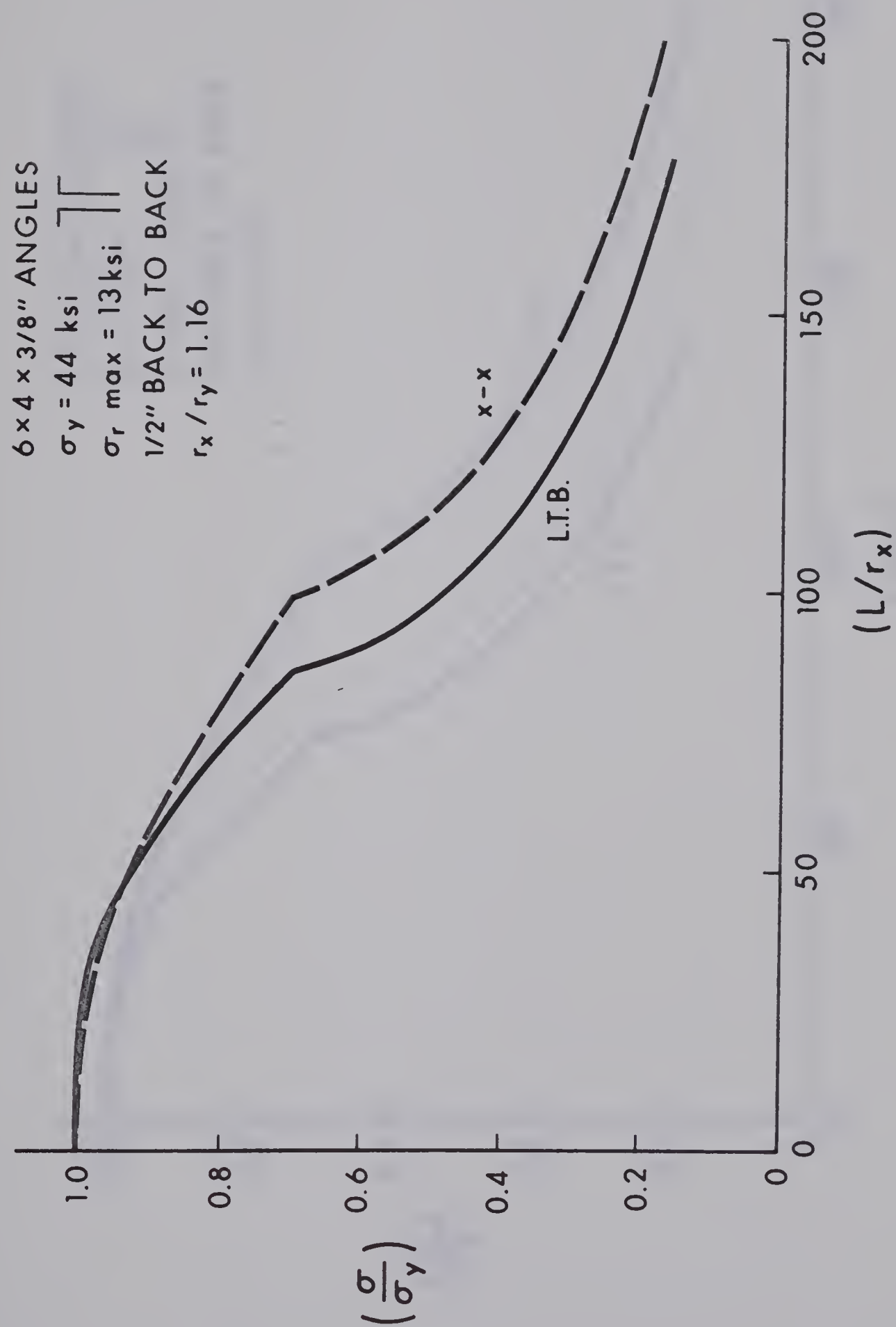


Figure 5.1d Influence of Member Asymmetry

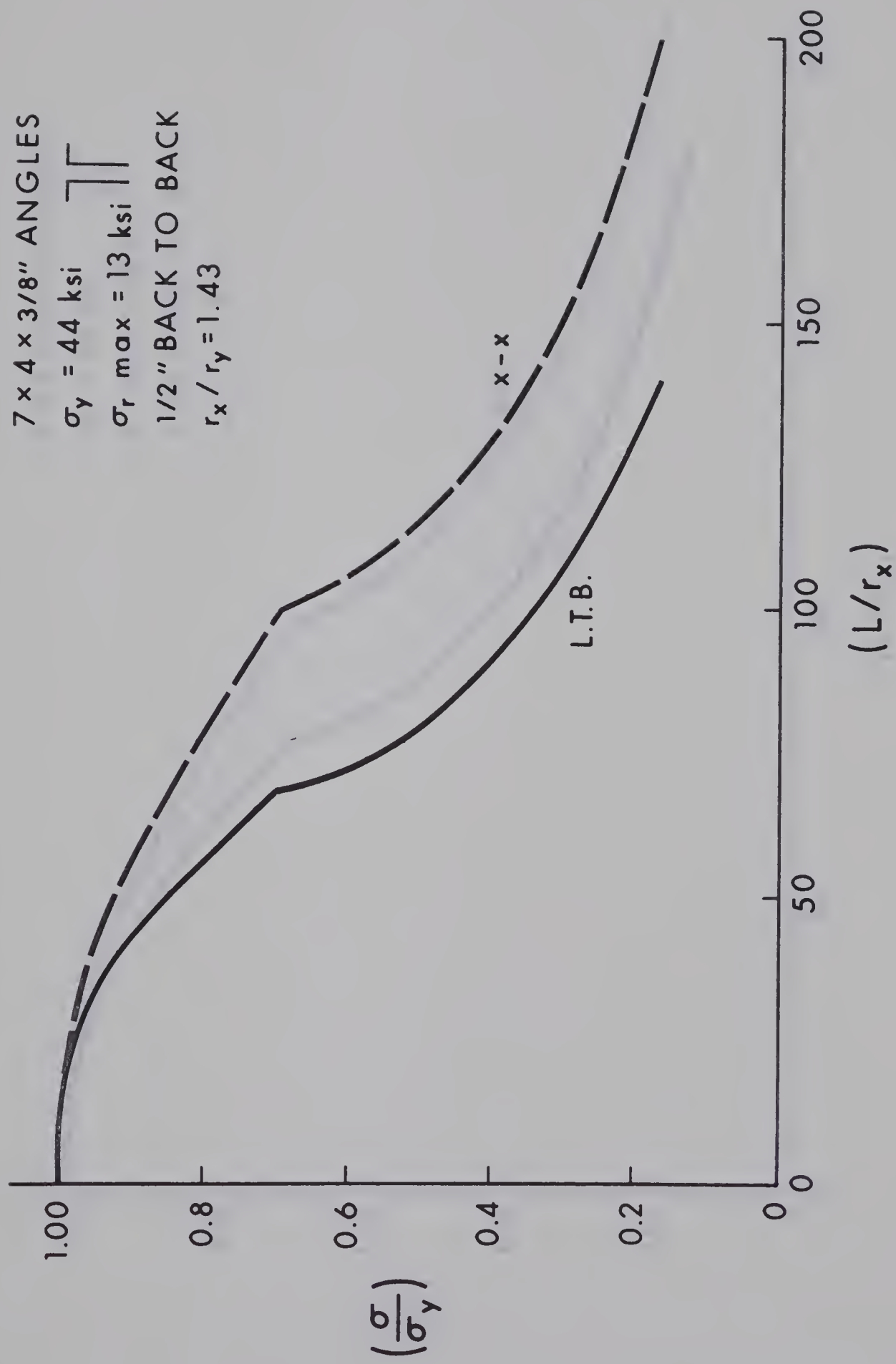


Figure 5.1e Influence of Member Asymmetry

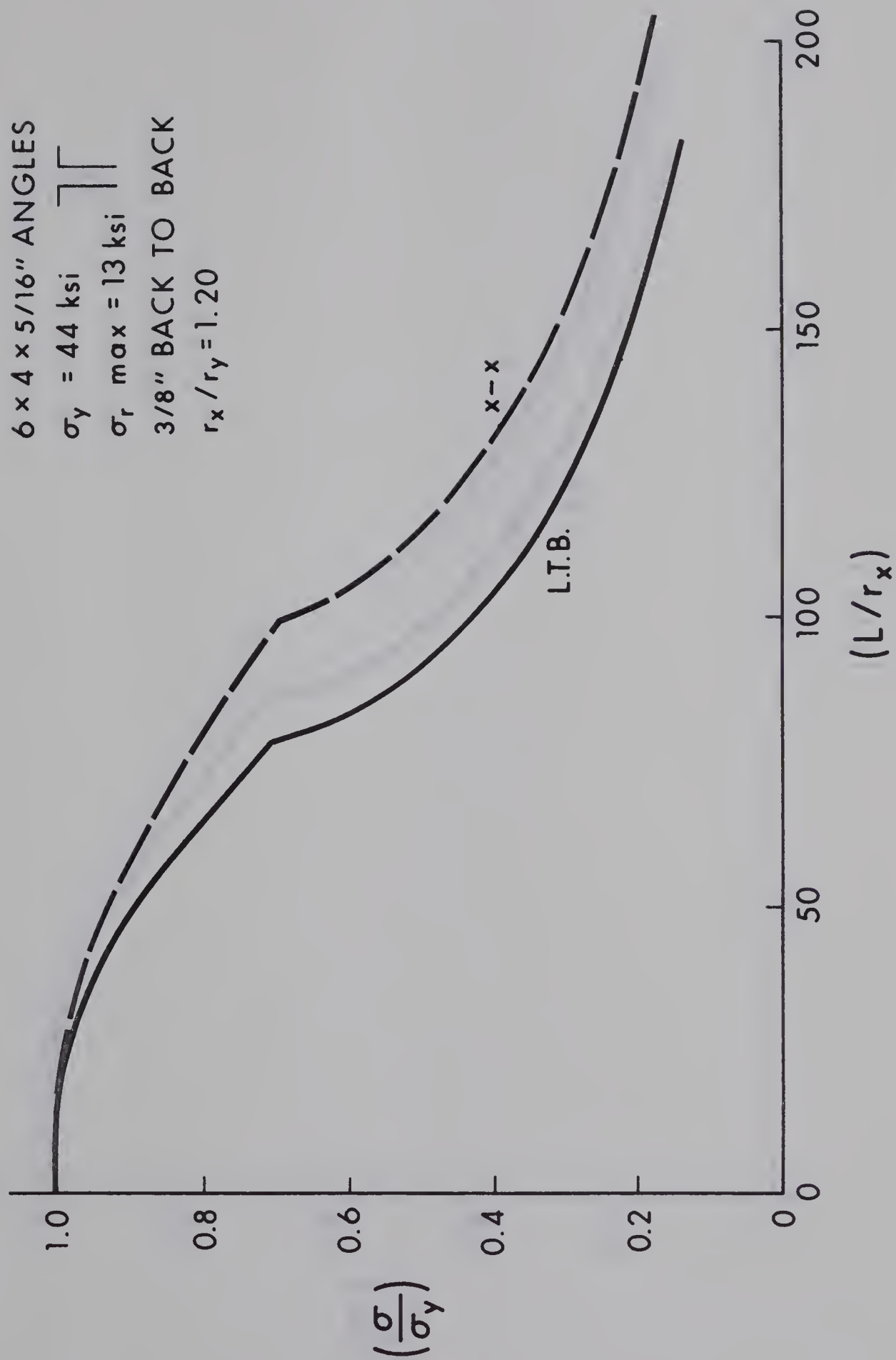


Figure 5.2a Influence of Leg Thickness

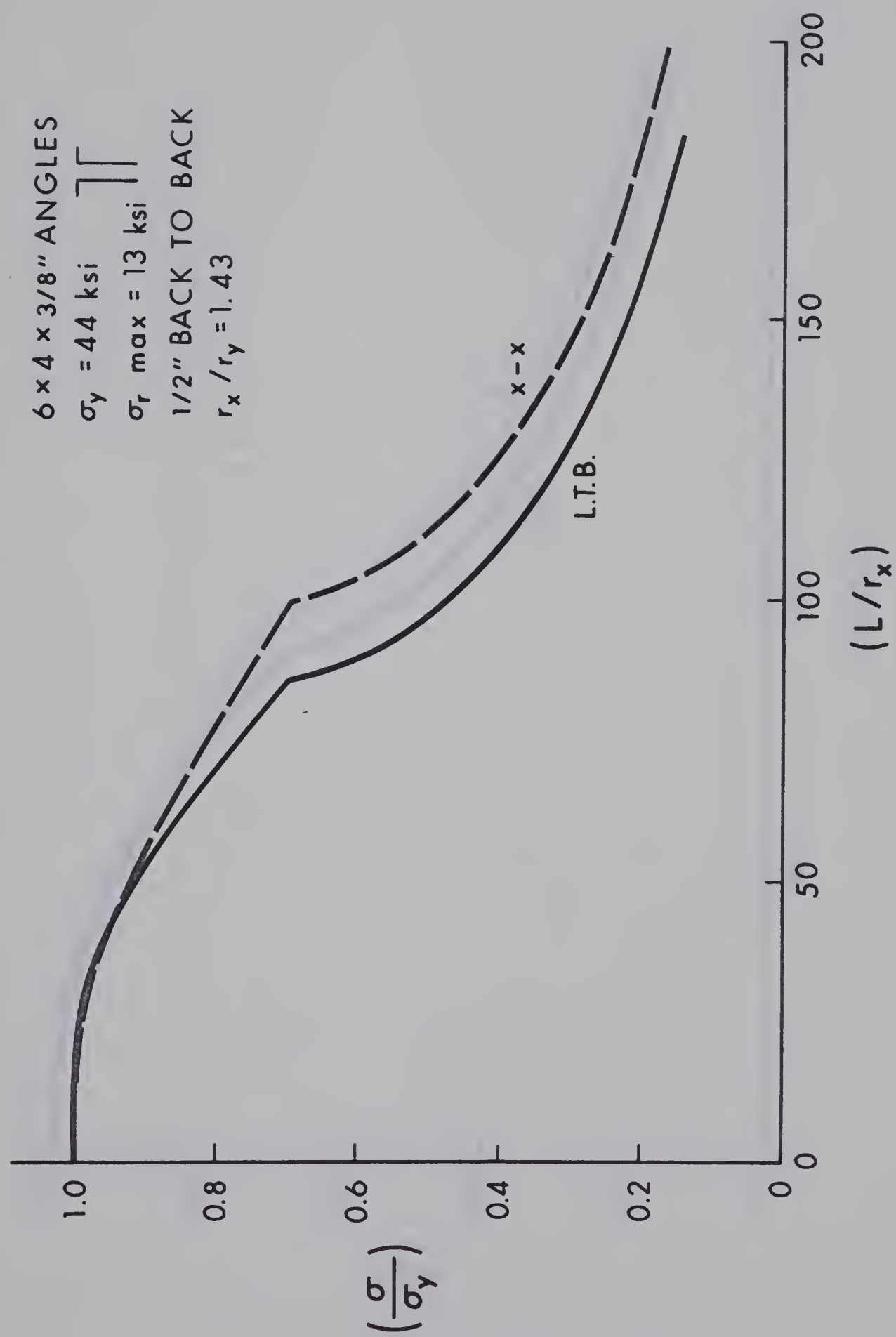


Figure 5.2b Influence of Leg Thickness

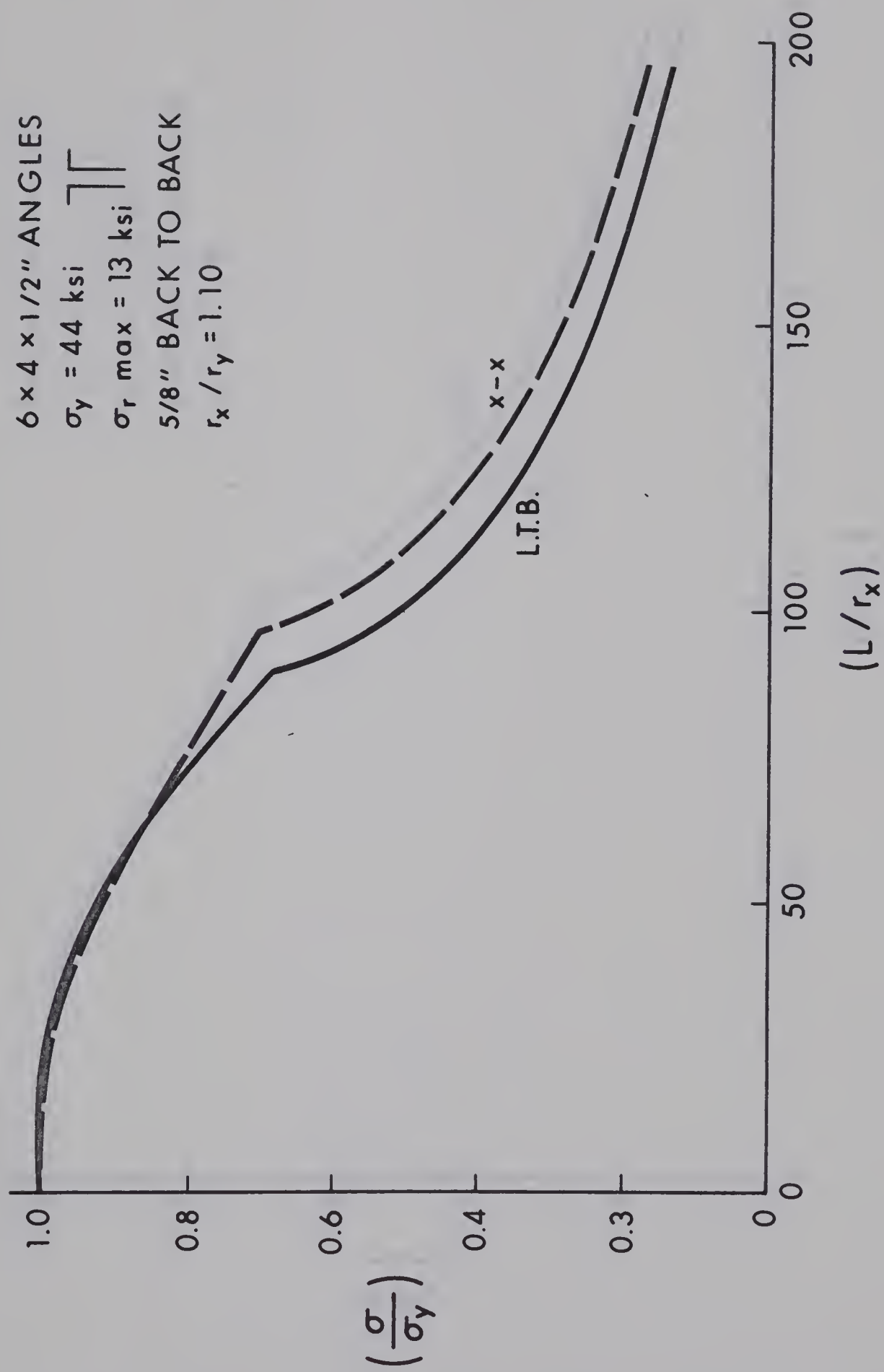


Figure 5.2c Influence of Leg Thickness

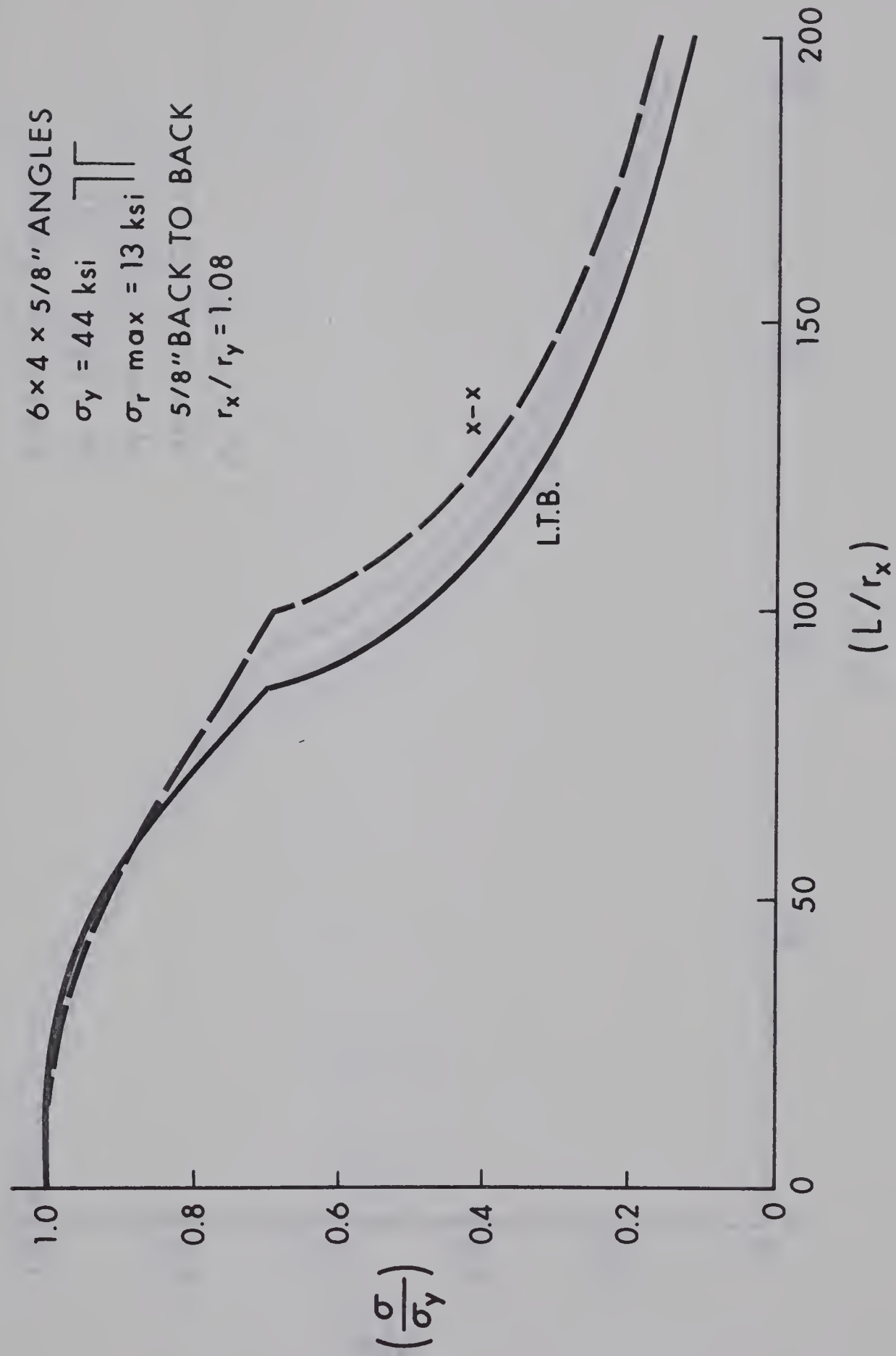


Figure 5.2d Influence of Leg Thickness

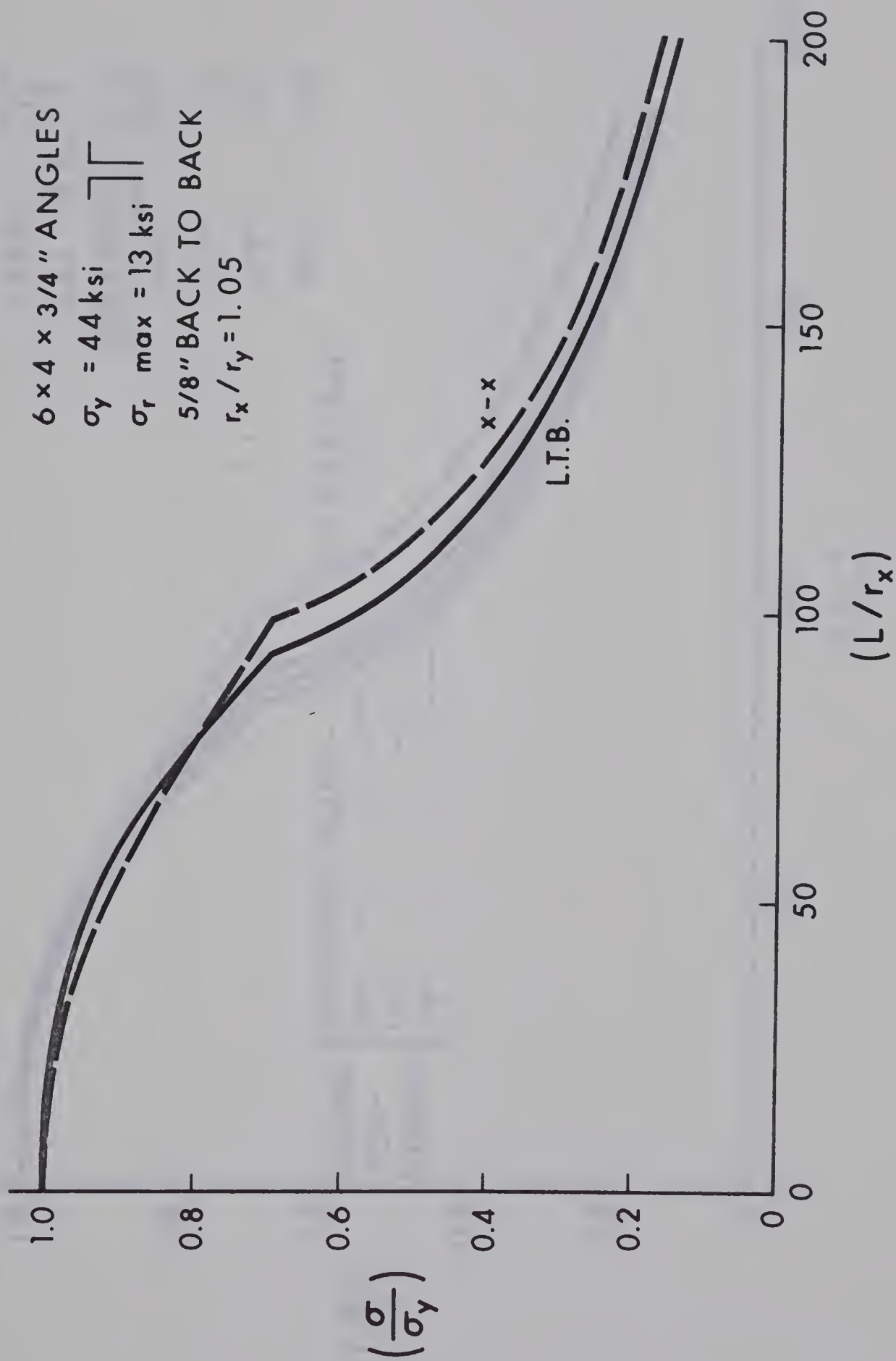


Figure 5.2e Influence of Leg Thickness

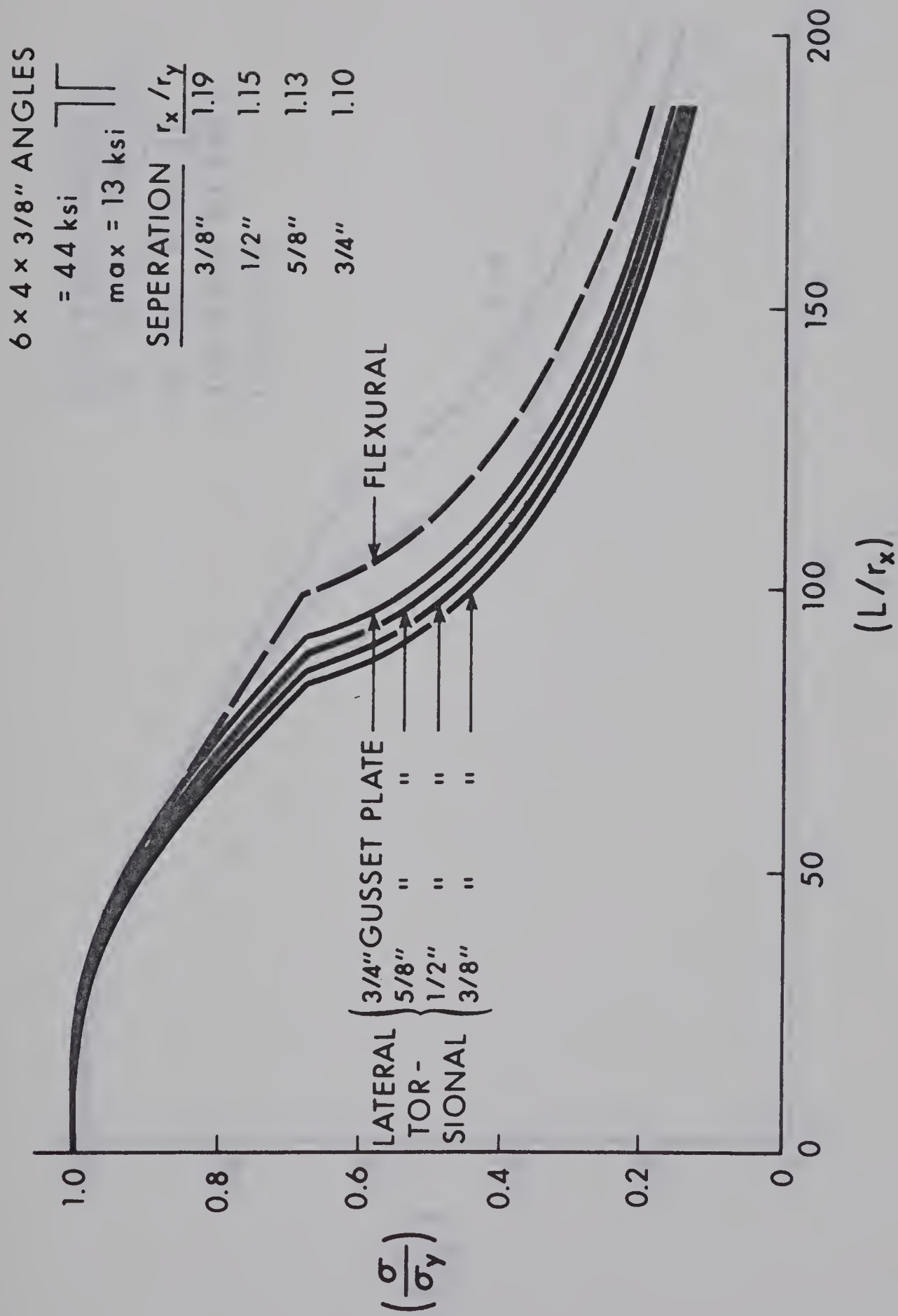


Figure 5.3 Influence of Leg Separation

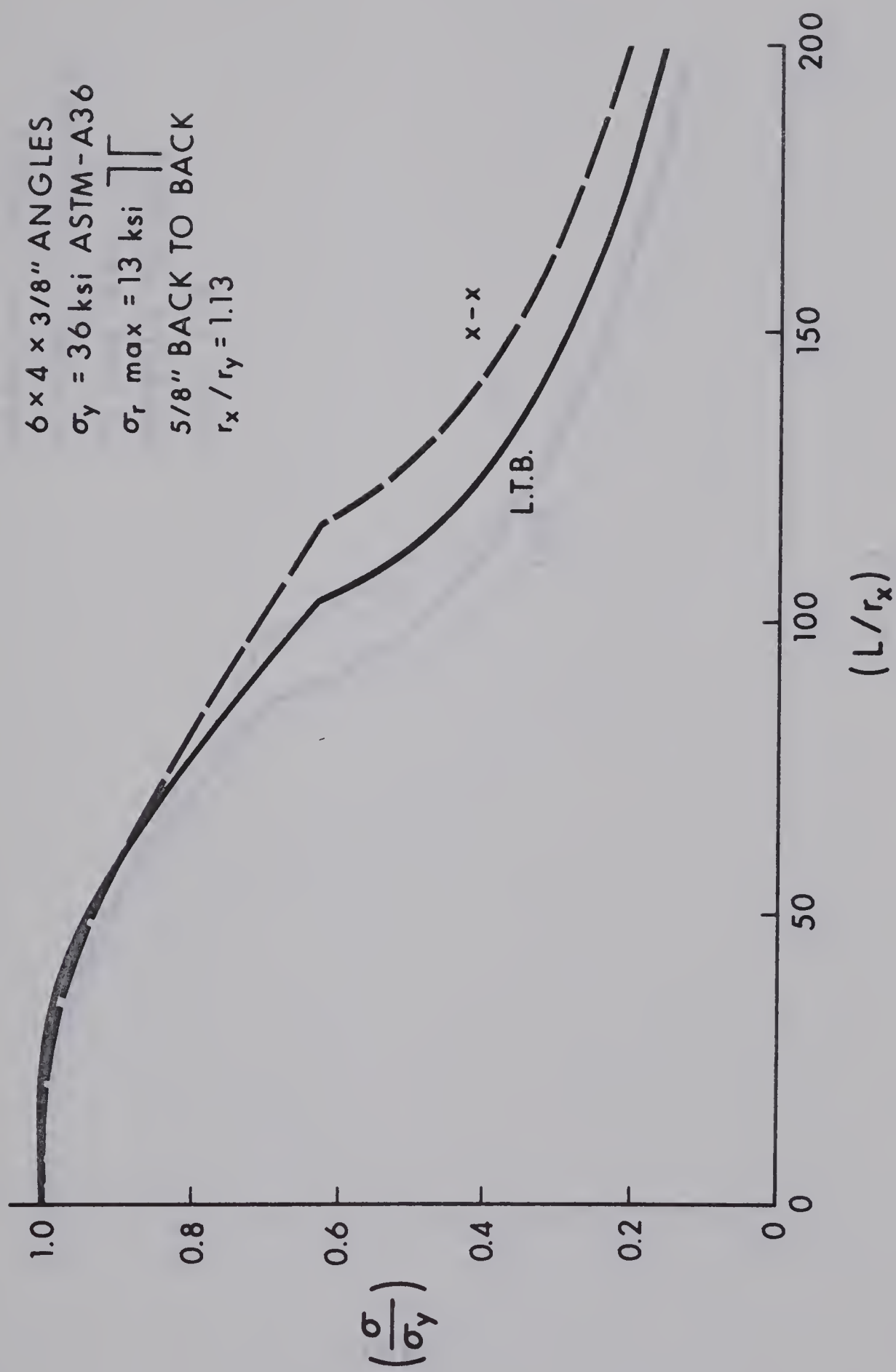


Figure 5.4a Influence of Yield Stress

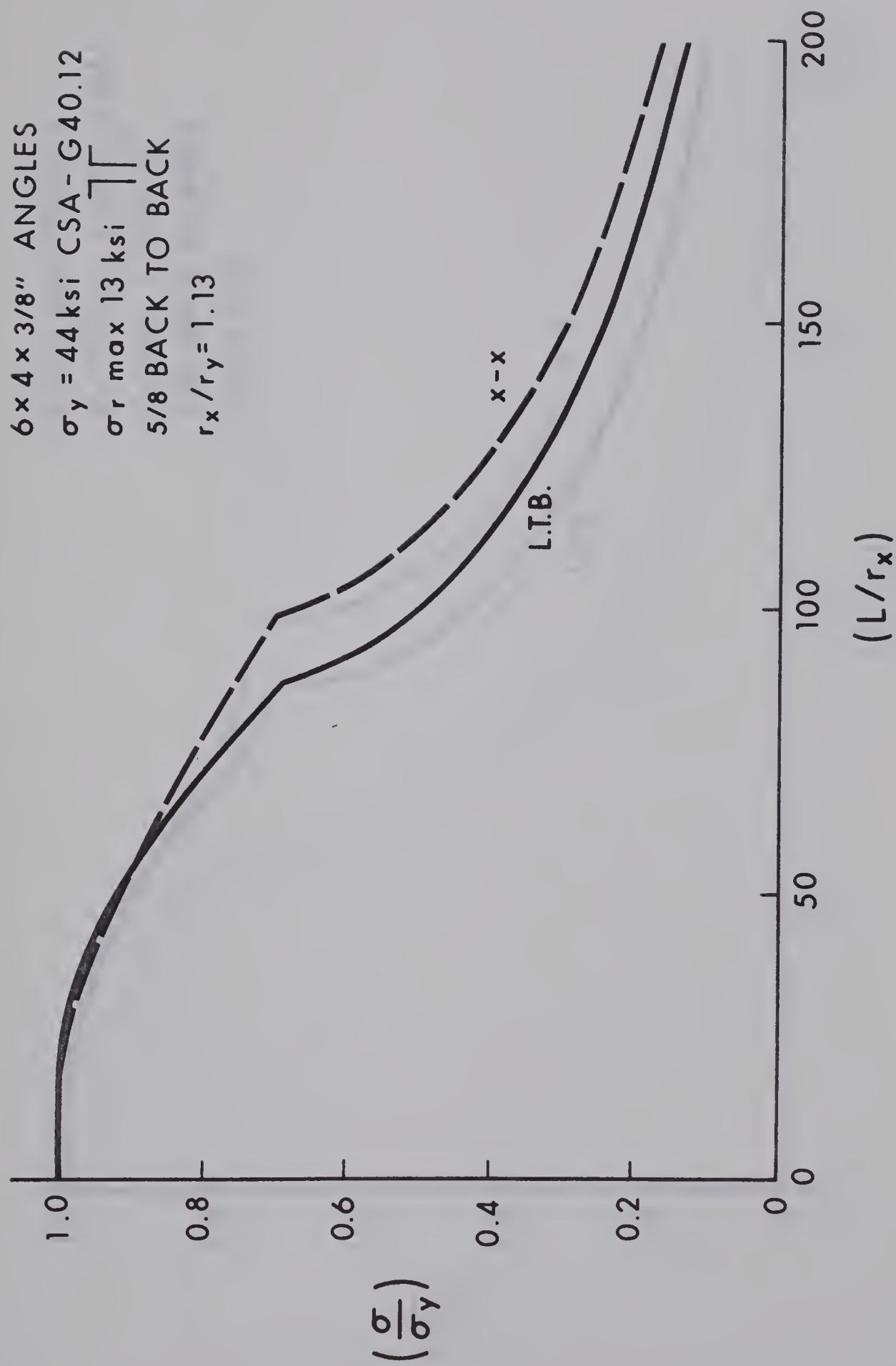


Figure 5.4b Influence of Yield Stress

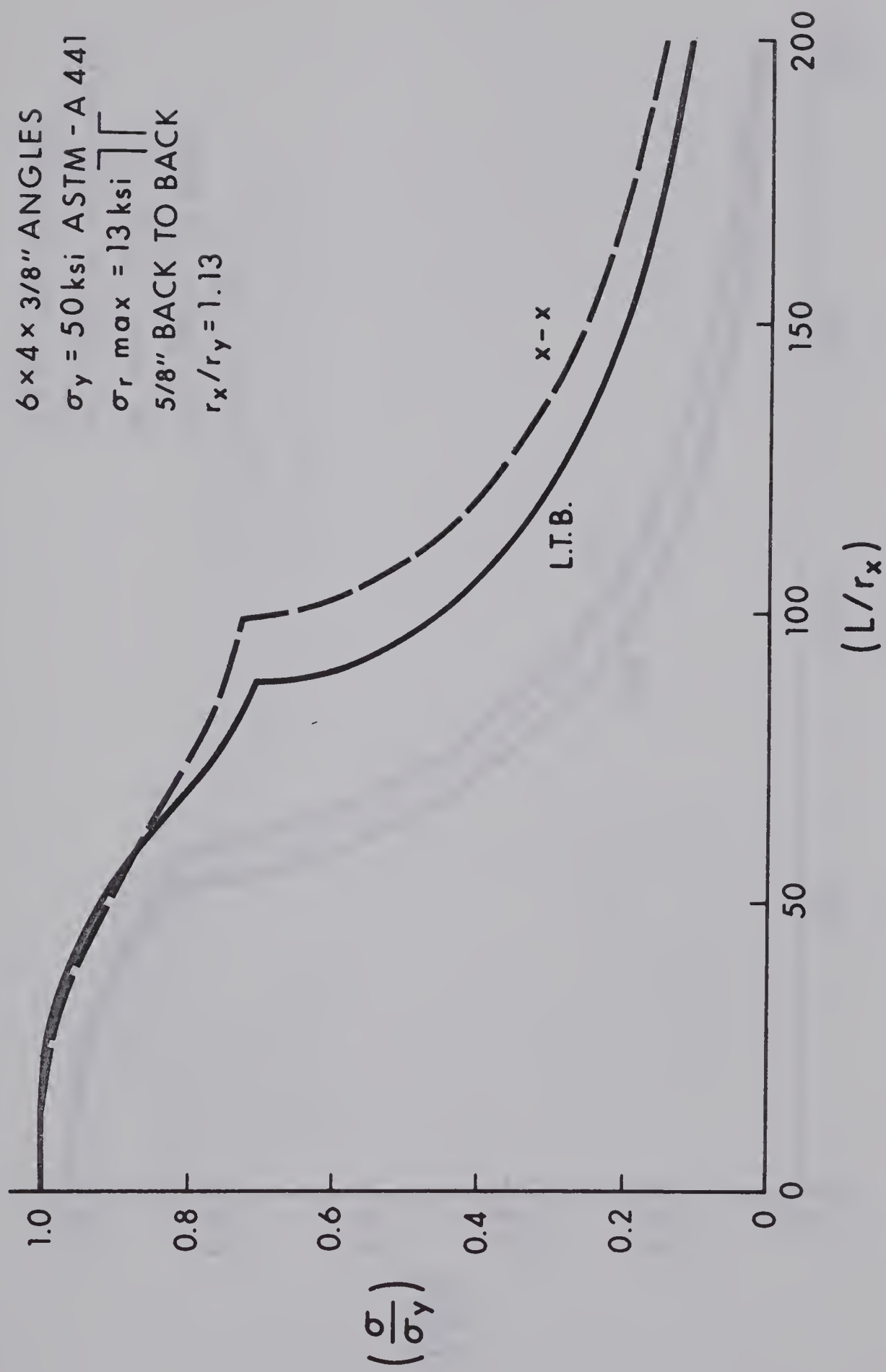


Figure 5.4c Influence of Yield Stress

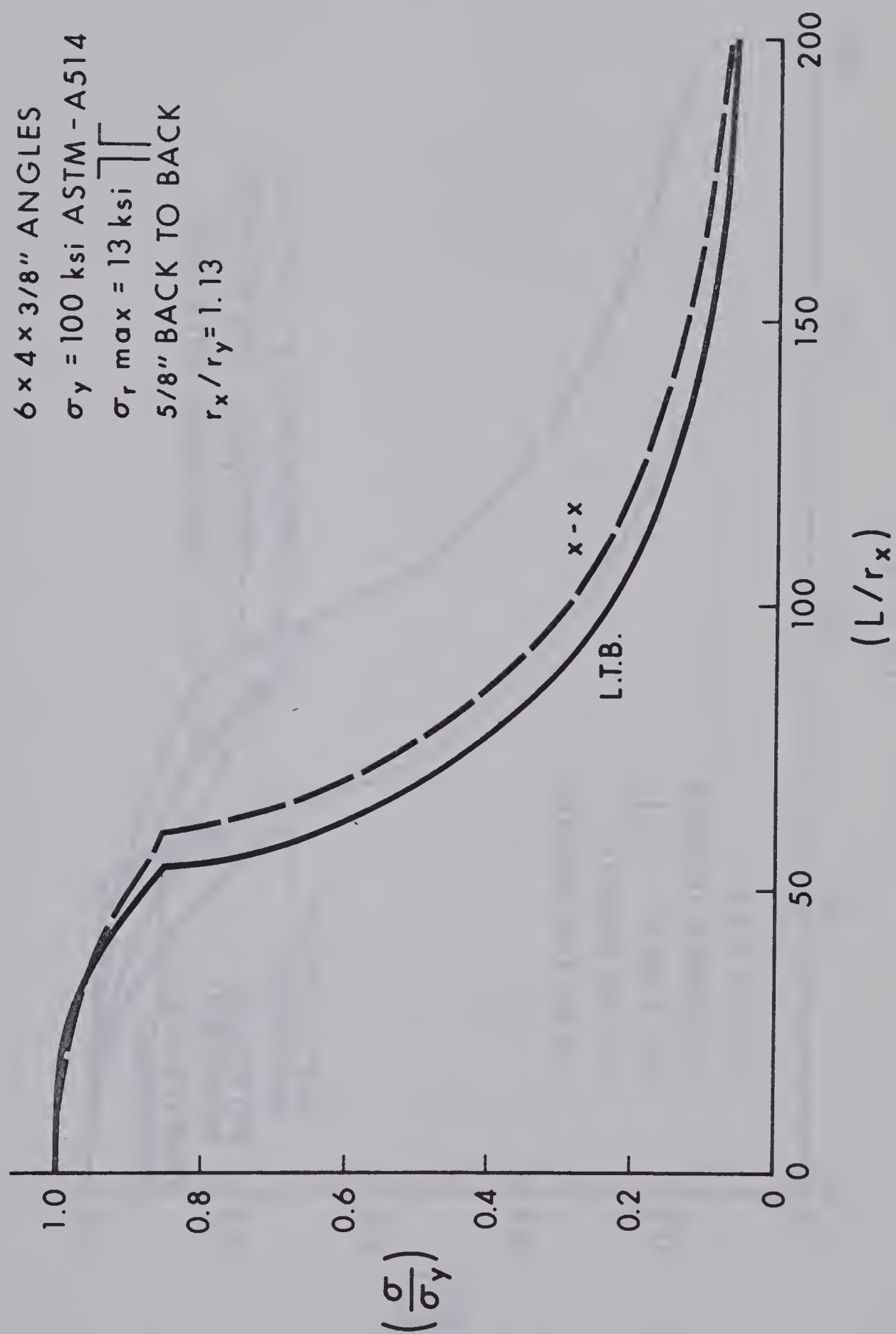


Figure 5.4d Influence of Yield Stress

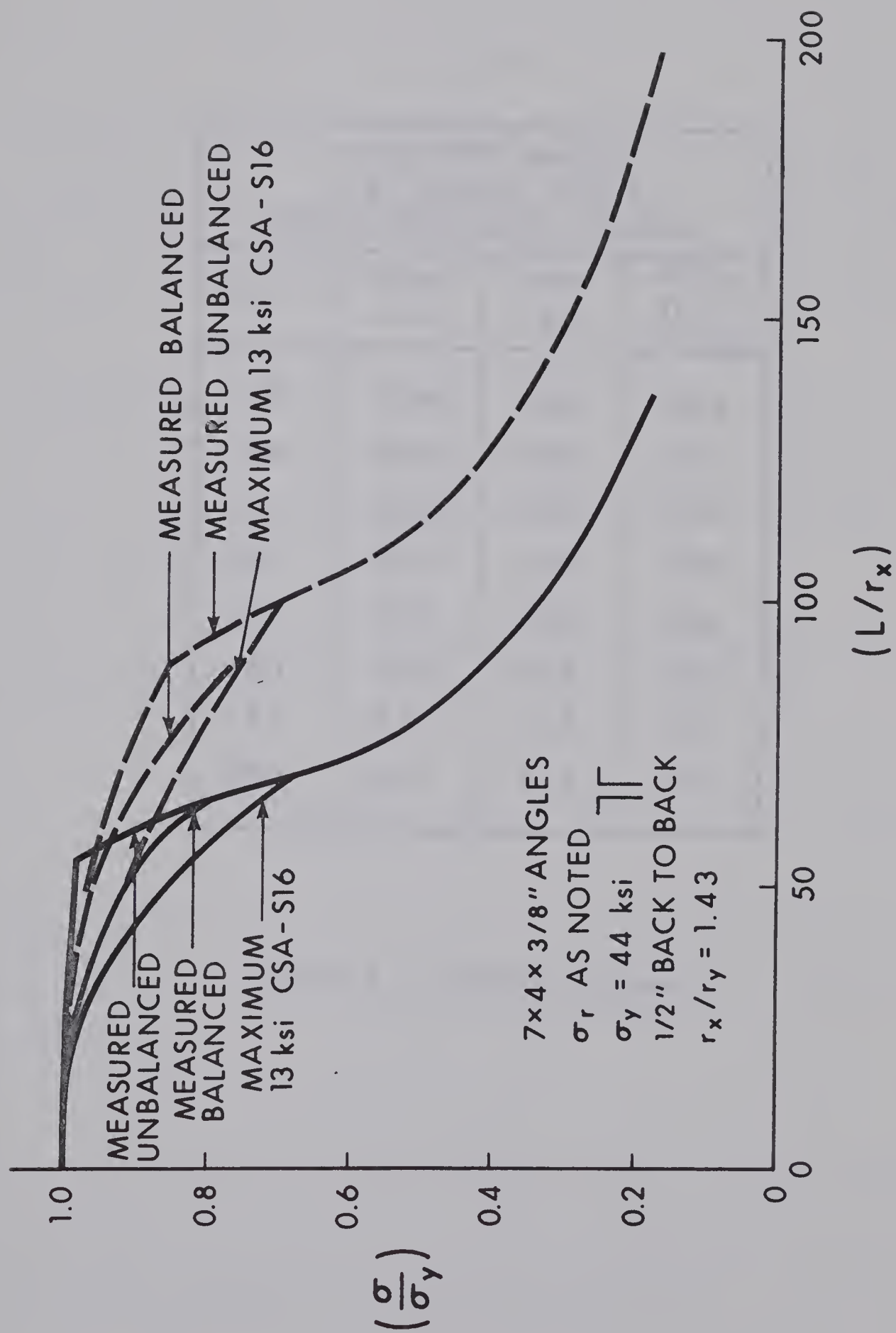


Figure 5.5 Influence of Residual Stress

6×4×3/8" ANGLE 5/8" GUSSET PLATE LONG LEGS BACK TO BACK			
L/r_x	σ/σ_y (x-x)	σ/σ_y (ϕy)	σ/σ_y (y-y) Fictitious
25	0.99	0.99	0.99
50	0.92	0.92	0.92
75	0.80	0.78	0.78
100	0.67	0.50	0.50
125	0.44	0.34	0.34
150	0.30	0.23	0.23
175	0.21	0.17	0.17
200	0.17	0.13	0.13

Table 5.1 Critical Stresses

CHAPTER VI

APPLICATION TO DESIGN

Procedures for the design of double angle struts are based on the assumption that flexural buckling will mark the ultimate strength of the member. The possibility of coupled flexural-torsional buckling is ignored.^(1,5)

The results of this investigation show that the lateral-torsional buckling load for a double angle strut, $P_{\phi y}$, is less than the y-y axis flexural buckling load, P_y , but the difference is within 2% for all cases investigated.

The virtual coincidence of $P_{\phi y}$ and P_y can be explained using Equation 4.2 as the basis;

$$-\frac{K}{P} (P-P_y)(P-P_{\phi}) - (P_{y_0})^2 = 0 \quad (6.1)$$

By neglecting the differential warping caused by the residual stresses and assuming that the stress on a particular fibre $\bar{\sigma} = P/A$, a quantity \bar{r}_0^2 can be defined as:

$$\bar{r}_0^2 = -\frac{\bar{K}}{P} = y_0^2 + \frac{I_x + I_y}{A} \quad (6.2)$$

Using this definition, Equation 6.1 can be rearranged as:

$$\frac{P}{P_{\phi}} + \frac{P}{P_y} - \left[1 - \frac{y_0^2}{r_0^2}\right] \frac{P^2}{P_{\phi} P_y} = 1 \quad (6.3)$$

with;

$$P_y = \frac{\pi^2 EI_y}{L^2} \quad (6.4)$$

and:

$$P_{\phi} = \frac{1}{r_0^2} [GK_T + \frac{\pi^2 EI_w}{L^2}] \quad (6.5)$$

a shape factor, J , can be defined as:

$$J = \left[1 - \frac{y_0^2}{r_0^2}\right] \quad (6.6)$$

where J is positive and always less than or equal to unity.

In the cases considered the warping resistance ($\frac{\pi^2 EI_w}{L^2}$) was significantly less than the St. Venant torsional resistance (GK_T). Neglecting the warping contribution and substituting the results of Equations 6.4 to 6.6 into Equation 6.3 the lateral torsional buckling load can be expressed as:

$$P_{\phi y} = \left[\frac{1 - (P_{r0}^2 / GK_T)}{1 - J(P_{r0}^2 / GK_T)} \right] \frac{\pi^2 EI_y}{L^2} \quad (6.7)$$

In Equation (6.7) the factor J reduces the value of the lateral-torsional buckling load below the (fictitious) y - y axis flexural buckling load.

For example, consider a $6 \times 4 \times \frac{3}{8}$ " double angle strut with $\frac{1}{2}$ " gusset plate and the long legs placed back to back. For a slenderness ratio, L/r_x , of 100 the warping torsional resistance is approximately 4% of the St. Venant resistance and can be neglected. The corresponding value of J is 0.97; this implies that $P_{\phi y}$ will be approximately 2% less than P_y . In the inelastic range at a slenderness ratio, L/r_x , of 50 the difference between the two loads is less than 1%. These results are typical of the cases considered.

In the design of a double angle strut, the column strength will be based on the lesser of the y - y and x - x axes buckling strengths. Since the y - y axis buckling strength virtually coincides with the lateral-torsional buckling strength, this procedure results in a correct assessment of the member strength.

The allowable stress procedure for column design restricts the computed stress on the member (under design loads) to a value obtained by dividing the critical stress (member strength) by a factor of safety. The factors of safety used in North American building codes are based on the buckling strength of rolled wide-flange members and have been checked against large-scale tests on such members.

The residual stress distribution for a double angle strut and its influence on the gradual plastification of the section may not be the same as that for a rolled wide-flange section. In order to assess the suitability of the above design provisions for double angle struts, the buckling strengths obtained from the computer analysis are

compared with the provisions of the CSA⁽⁵⁾ and AISC⁽¹⁾ standards in Figures 6.1 and 6.2.

Figure 6.1 and 6.2 plot the flexural and lateral-torsional buckling strengths respectively, for a $4 \times 3 \times \frac{3}{8}$ " double angle strut, placed with long legs back to back and separated by a $\frac{1}{2}$ " gusset plate. The material is CSA-G40.12 steel with a specified minimum 13 ksi (using the assumed distribution of Chapter III).

Figure 6.1 plots the critical stress for x-x axis flexural buckling, σ/σ_y , against the slenderness ratio, L/r_x ; whereas the curves representing lateral-torsional buckling, Figure 6.2, plot the critical stress against the y-y axis slenderness ratio, L/r_y , to simplify the comparisons. The computer solutions are shown as heavy solid curves with the CSA allowable stresses as lighter solid curves and the AISC allowable stresses as light broken lines. The factors of safety, based on comparisons of the flexural and lateral buckling strengths with the CSA and AISC design provisions are shown in Table 6.1.

In the elastic range these factors of safety are constant at 1.96. This value is normally taken as 1.92; the difference is the result of using $E = 29,600$ ksi in the computer program instead of the more conservative value of $E = 29,000$ ksi^{1,5}.

In the inelastic range the factors of safety provided by the CSA provisions decrease gradually from 1.96 at the elastic limit to 1.67 at a slenderness ratio of zero. The factors of safety provided by the AISC provisions increase from 1.96 at the elastic limit to

2.06 at a slenderness ratio of 100, then decrease gradually to 1.67 at a slenderness ratio of zero.

In Table 6.1, the critical stresses, σ_{cr} , as given by the Column Research Council's²⁰, basic column formula, are also listed; where

$$\sigma_{cr} = \sigma_y \left[1 - \left(\frac{\sigma_r}{\sigma_y} \right) \left(1 - \frac{\sigma_r}{\sigma_y} \right) \left(\frac{\sigma_y}{\pi^2 E} \right) \left(\frac{KL}{r} \right)^2 \right] \quad (6.8)$$

Using a peak compressive residual stress, σ_r of 13 ksi, the predictions of the CRC equation matched the computed flexural and lateral-torsional buckling stresses to within 1%.

Local buckling of the angle was not considered in this investigation. Column curves have been presented for angle sections having leg width-to-thickness ratios, b/t , exceeding the CSA requirement of $75/\sqrt{F_y}$ and the AISC requirement of $76/\sqrt{F_y}$, in order to investigate the significance of the various structural parameters. Where the leg width-to-thickness ratio exceeds the code limitation a reduction factor would be applied to the allowable stress to account for the possibility that local buckling of the plates which make up the cross-section may occur before overall buckling of the member.

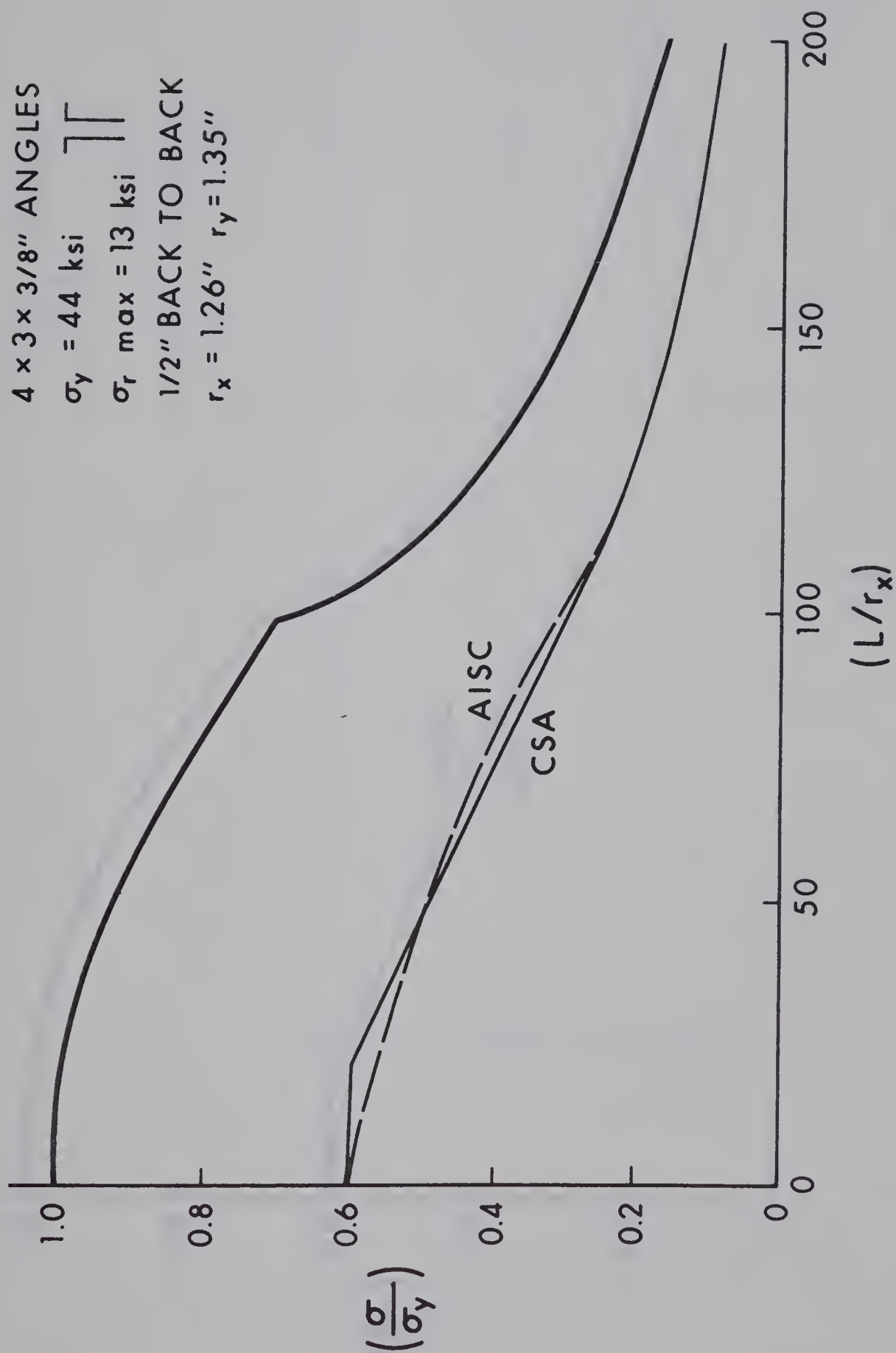


Figure 6.1 Ultimate and Design Curves Flexural Buckling

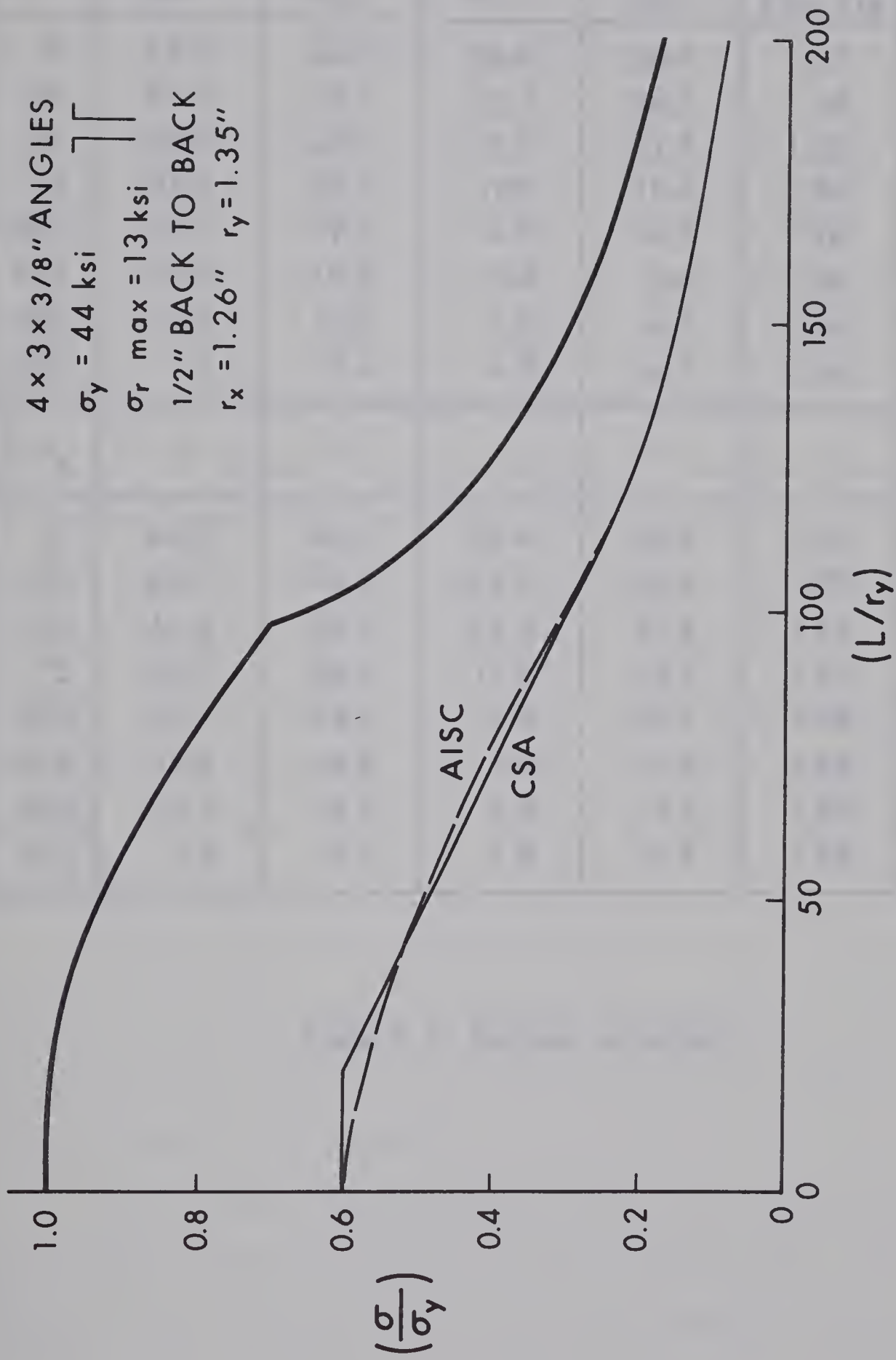


Figure 6.2 Ultimate and Design Curves Lateral-Torsional Buckling

L/r_x	COMPUTED ULTIMATE STRENGTH (KSI)	COLUMN RESEARCH COUNCIL (KSI)	CSA - S16 (DESIGN) (KSI)	AISC (DESIGN) (KSI)	COMPUTED FACTOR OF SAFETY	
					ULT. STR. CSA-S16	ULT. STR. AISC
0	44.0	44.0	26.4	26.4	1.67	1.67
25	43.5	43.2	25.7	24.5	1.69	1.78
50	40.0	40.0	22.3	21.8	1.80	1.83
75	35.6	35.6	19.0	18.4	1.88	1.94
100	29.2	29.2	14.9	14.2	1.96	2.06
125	18.8	18.8	9.6	9.6	1.96	1.96
150	12.9	12.9	6.6	6.6	1.96	1.96
175	9.6	9.6	4.9	4.9	1.96	1.96
L/r_y	"	"	"	"	"	"
0	44.0	44.0	26.4	26.4	1.67	1.67
25	43.7	43.2	25.7	24.5	1.70	1.78
50	41.8	40.5	22.3	21.8	1.87	1.92
75	36.3	36.4	19.0	18.4	1.91	1.97
100	29.2	29.2	14.9	14.2	1.96	2.06
125	18.8	18.8	9.6	9.6	1.96	1.96
150	12.9	12.9	6.6	6.6	1.96	1.96
175	9.6	9.6	4.9	4.9	1.96	1.96

Table 6.1 Factors of Safety

CHAPTER VII

SUMMARY AND CONCLUSIONS

This investigation attempts to define the flexural and lateral-torsional buckling strengths of double angle struts.

Residual stress distributions were measured on five angle sections of CSA-G40.12 steel and are presented in Figures 3.1(a) to 3.1(3); along with the corresponding material properties.

The residual stress distribution was idealized and used in a computer program to predict the flexural and lateral-torsional buckling strengths. The cross-section properties calculated were based on the elastic core of the cross-section remaining at each stage of loading. In the computations, the two angles composing the member were assumed to be joined by a thin strip of material located at the gauge line. This implies that the two angles act as a unit to resist the buckling motions.

Column curves are plotted as Figures 5.1 to 5.5 and illustrate the influence of; member asymmetry, leg thickness, leg separation, yield stress and residual stresses on the flexural and lateral-torsional buckling strengths of the member.

In all cases investigated the lateral-torsional buckling load, $P_{\phi y}$, was within 2% of the y-y axis flexural buckling load. This is because the shape factor, J , for double angle sections is approximately

equal to one, throughout the complete loading range.

The flexural and lateral-torsional buckling strengths compare favorably with predictions given by the CRC basic column strength equation. In addition the same factors of safety required by the CSA and AISC building codes for rolled wide flange sections are achieved by double angle sections designed only on the basis of flexural buckling.

The design of double angle struts considering only the strong and weak axis buckling strengths is satisfactory, since the lateral-torsional buckling strength is within 2% of the y-y axis buckling strength normally computed by the designer.

NOMENCLATURE

A	Cross sectional area
E	Modulus of elasticity
E_{st}	Strain-hardening modulus
FS	Factor of safety
g	Gauge location
G	Shear modulus
I	Moment of inertia
I_w	Warping moment of inertia
J	Shape factor
\bar{K}	Differential warping reduction
K_T	St. Venant torsional constant
L	Length
P	Applied load
P_c	Critical buckling load
P_x	Flexural buckling load X-X axis
P_y	Flexural buckling load Y-Y axis
$P_{\phi y}$	Lateral-torsional buckling load
P_{ϕ}	Torsional buckling load
r	Radius of gyration
r_0	Polar radius of gyration
u	Displacement in x direction

v	Displacement in y direction
X_0	X coordinate of shear centre from centroid
Y_0	Y coordinate of shear centre from centroid
ϵ	Strain
ϵ_a	Applied strain
ϵ_r	Residual strain
ϵ_{st}	Strain at onset strain-hardening
ϵ_t	Total strain
ϵ_y	Yield strain
ϕ	Rotation
σ	Stress
σ_a	Applied stress
σ_c	Critical buckling stress
σ_r	Residual stress
σ_t	Total stress
σ_y	Yield stress

LIST OF REFERENCES

1. A.I.S.C. - "Specification for the Design, Fabrication and Erection of Structural Steel for Buildings," American Institute of Steel Construction, 1969.
2. A.S.T.M. - "Mechanical Testing of Steel Products," American Society for Testing Materials Standard A370-65.
3. Beedle, L.S. and L. Tall, - "Basic Column Strength," Lehigh University, Fritz Laboratory Report No. 220A.34, September, 1959.
4. Beedle, L.S., T.V. Galambos, and L. Tall - "Structural Steel Design," Ronald Press Company, New York, 1968.
5. C.I.S.C. - "Handbook of Steel Construction," Canadian Institute of Steel Construction, 1967.
6. Chajes, A. and G. Winter - "Torsional Flexural Buckling of Thin Walled Members," Proc. ASCE, Vol. 94, ST8, August, 1968.
7. C.S.A. - "General Purpose Structural Steel," Canadian Standards Association, Standard G40.12, 1964.
8. Galambos, T.V. - "Structural Members and Frames," Prentice-Hall Inc., Englewood Cliffs, N.J., 1968.
9. Galambos, T.V., N.S. Trahain and T. Usami - "Eccentrically Loaded Single Angle Columns," Washington University, Structural Division, Research Report No. 11, 1969.
10. Godfrey, G.B. - "The Allowable Stress in Axially Loaded Steel Struts," The Structural Engineer, Vol. 40, No. 3, March, 1962.
11. Huber, A.W. and L.S. Beedle, - "Residual Stress and the Compressive Strength of Steel," Welding Journal, Research Supplement, Vol. 33, No. 12, December, 1954.
12. Jhamb, I.C., W.H. Jones, M.K. Wilkinson and J.H. Wynhoven - "Discussion, Inelastic Torsional Buckling of H-Columns," Proc. ASCE, Vol. 94, ST8, August, 1968.

13. Johnston, B.G. and F. Opila - "Compression and Tension Tests of Structural Alloys," Proc. A.S.T.M., Vol. 41, 1941.
14. Johnston, B.G. - "Guide to Design Criteria for Metal Compression Members," Column Research Council, Wiley and Sons, New York, 1966.
15. Johnston, B.G. - "Pin Connected Plate Links," Trans. ASCE, Vol. 104, 1939.
16. Lee, G.C., D.S. Fine, W.R. Has "Inelastic Torsional Buckling of H-Columns," Proc. ASCE, Vol. 93, ST5, October, 1967.
17. Lenzen, K.H. - "Design Formula for the Top Chord of Open Web Steel Joists," University of Kansas, Studies in Engineering Mechanics, Report No. 27.
18. O'Connor, C. - "Residual Stresses and Their Influence on Structural Design," Journal of the Institute of Engineers, Australia, Vol. 27, 1955.
19. Shanley, F.R. - "Inelastic Column Theory," Journal Aeronautical Science, Vol. 14, No. 5, May, 1947.
20. Sherman, D.R. - "Residual Stress Measurements in Tubular Members," Proc. ASCE, Vol. 95, ST4, April, 1969.

APPENDIX A

LEVEL 17 (1 NOV 68)

OS/360 FORTRAN H

```

COMPILER OPTIONS - NAME= MAIN,OPT=02,LINECNT=59,SOURCE,FBCDIC,NOLIST,NODFCK,LOAD,
INTEGER OUTPUT , D1 , D2, D3, M , N, H          NOMAP,NOFDIT,ID,NOXREF]
C   DEFINE CARD READER NUMBER
    INPUT = 5
C   DEFINE PRINTER UNIT NUMBER
    OUTPUT = 6
    REAL L1,L2,L3,LOAD,IXX,IYY,LRX,LRY,IWY,IWX,IW,LL1,LL2
    DIMENSION SR1(90),SR2(90),SR3(5),WO(500),WN(500),WNN(500),AIW(500)
    LOAD = 0.0
    IXX = 0.0
    IYY = 0.0
    A = 0.0
    AD = 0.0
C   READ MATERIAL PROPERTIES IN KSI.
    READ(INPUT,1)E,STRESY,G
    1 FORMAT(3F10.2)
    SY = STRESY / F
C   READ MEMBER SIZES IN IN. AND DIVISIONS REQUIRED (AS PER CSA-S16)
    READ(INPUT,2) L1,T1,D1,L2,T2,D2,L3,T3,D3,K
    2 FORMAT ( 3 (2F5.2,I5) ,I2)
C   REDEFINE NEW LENGTHS ADJUST DIMENSIONS TO CENTRE LINE
    L1=L1-T2/2.
    L2=L2-T1/2.
    L3=L3+T2
    AL1=L1/D1
    AL2=L2/D2
    AL3=L3/D3
    GAUGE=K*AL2
C   READ ALL RESIDUAL STRAINS INDIVIDUALLY
    READ(INPUT,3) (SR1(I),I=1,D1)
    3 FORMAT ( 8F10.8 )
    READ(INPUT,3)(SR2(I),I=1,D2)
    READ(INPUT,3)(SR3(I),I=1,D3)
C   PRINT HEADINGS AND DATA INPUT
C   READ ONE VALUE OF APPLIED STRAIN
    10 READ(INPUT,4,FND=999)SA
    4 FORMAT ( F10.8)
    WRITE(OUTPUT,20)
    20 FORMAT('1',51X, 'CIVIL ENGINEERING DEPARTMENT' / 54X ,
    1'UNIVERSITY OF ALBERTA' // 32X , 'ANALYSIS OF RESIDUAL STRAINS IN D
    2DOUBLE ANGLE COMPRESSION MEMBERS' //
    WRITE(OUTPUT,21) E , STRESY , SY
    21 FORMAT( 9X, 'MATERIAL PROPERTIES' // 14X , 'MODULUS OF ELASTICITY
    1 = ', F10.2 , ' KSI.' // 14X , 'YIELD STRESS', 11X, '= ', F10.2 ,
    2 ' KSI.' // 14X , 'YIELD STRAIN', 11X, '= ', F10.8 , ' IN/IN' //
    WRITE(OUTPUT,22) D1,T1,L1,D2,T2,L2,D3,T3,L3,GAUGE
    22 FORMAT( 9X, 'STRUCTURE TOPOLOGY' // 20X , 'MEMBER', 18X, 'NUMBER OF
    1' , 12X , 'THICKNESS' , 12X , 'LENGTH' / 16X , 'NAME' , 6X , 'NUMBER',
    2 12X , 'DIVISIONS' , 14X , 'INCHES' , 13X , 'INCHES' // 14X ,
    3 'FREE LEGS      1' , 18X , I3 , 17X , F5.3 , 14X , F5.3 // 14X,
    4 'JOINED LEGS    2' , 18X , I3 , 17X , F5.3 , 14X , F5.3 // 14X,
    5 'JOINER         3' , 18X , I3 , 17X , F5.3 , 14X , F5.3 // 14X,
    6 'GAUGE LENGTH = ', F5.3 , ' IN' // )
C   GAUGE LENGTH MEASURED FROM CENTRE LINE SECTION ONE
    WRITE(OUTPUT,23)
    23 FORMAT ( 9X, 'RESIDUAL STRAINS (COMPRESSION POSITIVE)'// 14X ,
    1 5('MEM DIV      STRAIN      ') )
    WRITE(OUTPUT,25)(( I, SR1(I)),I=1,D1)
    25 FORMAT (15X , 5('1', 2X,I3,2X, F10.8, 4X )/
    1(15X,5('1',2X,I3,2X,F10.8,4X)))
    WRITE(OUTPUT,27)((I ,SR2(I)),I=1,D2)
    27 FORMAT (15X , 5('2' , 2X,I3 , 2X, F10.8, 4X )/
    1(15X,5('2',2X,I3,2X,F10.8,4X)))
    WRITE(OUTPUT,29)((I, SR3(I)), I=1,D3)
    29 FORMAT (15X , 5('3', 2X ,I3 , 2X, F10.8,4X )/
    1(15X,5('2',2X,I3,2X,F10.8,4X)))
    WRITE(OUTPUT,30) SA
    WRITE(OUTPUT,20)
    30 FORMAT( 9X , 'APPLIED STRAIN =' , F10.8 , 'IN/IN' //
    WRITE(OUTPUT,31)
    31 FORMAT( 9X , 'PORTIONS OF SECTION YIELDED DUE TO RESIDUAL STRAIN'
    1 // 20X , 'MEMBER' , 10X , 'DIVISION' , 10X , 'TOTAL' / 20X,
    2 'NUMBER' , 11X , 'NUMBER' , 10X , 'STRAIN' / )
C   TEST FOR YIELDED SECTIONS AND COMPUTE LOCATION OF X-X AXIS
C   CALCULATE IYY
C   SECTION 1
    YB=L3/2.
    DO 50 I=1,D1
    ST=SA+SR1(I)
    IF(ST.GE.SY)ST=SY
    LOAD=LOAD+2.*ST*E*T1*AL1
    IF(ST.GF.SY)GO TO 50
    XBAR=YB+L1-(I*AL1)+AL1/2.
    IYY=IYY+2.*(( T1*AL1 **3/12.)+(T1*AL1*XBAR**2))
    A=A+2.*T1*AL1
    50 CONTINUE

```



```

C SECTION 2
  DO 150 I=1,D2
    ST=SA+SR2(I)
    IF(ST.GE.SY)ST=SY
    LOAD=LOAD+2.*ST*E*T2*AL2
    IF(ST.GE.SY)GO TO 150
    XBAR=YB
    IYY=IYY+2.*((AL2*T2**3 /12.)+(AL2*T2*XBAR**2))
    AD=AD+2.*(AL2*T2*(L2-I*AL2+AL2/2.))
    A=A+2.*AL2*T2
  150 CONTINUE
C SECTION 3
  DO250 I=1,D3
    ST=SA+SR3(I)
    IF(ST.GE.SY)ST=SY
    LOAD=LOAD+ST*E*T3*AL3
    IF(ST.GE.SY)GO TO 250
    XBAR=ABS(YB-I*AL3+AL3/2.)
    IYY=IYY+((T3*AL3**3/12.)+(AL3*T3*XBAR**2))
    AD=AD+AL3*T3*GAUGE
    A=A+AL3*T3
  250 CONTINUE
  YBAR=AD/A
  YAREA=A
C CALCULATE IXX
C SECTION 1
  DO 300 I=1,D1
    T=T1
    ST=SA+SR1(I)
    IF(ST.GE.SY)T=0.
    D=YBAR
    IXX=IXX+2.*((AL1*T**3/12.)+(AL1*T*D**2))
  249 FORMAT(5X,'T=',F12.4,3X,'D=',F12.4,3X,'IXX=',F12.4/)
  300 CONTINUE
  T=T2
C SECTION 2
  DO310 I=1,D2
    T=T2
    ST=SA+SR2(I)
    IF(ST.GE.SY)T=0.
    D=ABS(L2-YBAR-I*AL2+AL2/2.)
    IXX=IXX+2.*((T*AL2**3/12.)+(AL2*T*D**2))
  310 CONTINUE
  T=T3
C SECTION 3
  DO320 I=1,D3
    T=T3
    ST=SA+SR3(I)
    IF(ST.GE.SY)T=0.0
    D=ABS(GAUGE-YBAR)
    IXX=IXX+((AL3*T**3/12.)+(AL3*T*D**2))
  320 CONTINUE
C CALCULATE FLEXURAL BUCKLING X AND Y AXES
  RXX =(IXX/A)**0.5
  RYY =(IYY/A)**0.5
  XLCR=(3.14159*3.14159*E*IXX/LOAD)**0.5
  YLCR=(3.14159*3.14159*E*IYY/LOAD)**0.5
  LRX = XLCR / RXX
  LRY = YLCR / RYY
C OUTPUT SECTION PROPERTIES
  WRITE(OUTPUT,400)
  400 FORMAT(9X,'PROPERTIES OF SECTION NOT YIELDED' //)
  WRITE(OUTPUT,401) IXX , IYY , LOAD , YBAR,
    1 RXX , RYY , XLCR , YLCR , LRX , LRY
  401 FORMAT( 14X,'IXX = ',F7.2,' IN-4' // 14X,'IYY = ',F7.2,
    1' IN-4' // 14X,'LOAD = ',F10.2,' KIPS' // 14X,'YBAR = ',
    2, F5.2,' IN.' //
    314X,'RX = ',F7.2,' IN.' //
    414X,'RY = ',F7.2,' IN.' //
    514X,'CRITICAL LENGTH XX AXIS = ',F7.2,' IN' //
    614X,'CRITICAL LENGTH YY AXIS = ',F7.2,' IN' //
    714X,'L/R X AXIS = ',F7.2 //
    814X,'L/R Y AXIS = ',F7.2 // )
C CALCULATE KT ON ELASTIC SECTION ONLY
  AKT=0.0
  AKT=AKT+(2./3.*L1)*(T1**3)
  AKT=AKT+(2./3.*L2)*(T2**3)
  AKT=AKT+(1./3.*L3)*(T3**3)
  WRITE(OUTPUT,603)AKT
  603 FORMAT(10X,'KT = ',F10.6//)
  GAUGE = GAUGE
  XAXIS = YBAR
  OMEGA = 0.
  IWX = 0.
  IWY = 0.
  BARK=0.0

```



```

C CALCULATE OMEGA SECTION 1
DO 533 I =1,D1
OM1 = OMEGA
OMEGA=OMEGA-AL1*XAXIS
T = T1
ST = SA+SR1(I)
IF(ST.GE.SY)T = 0.
Y1 = XAXIS
X1=-L1-YB+(I-1)*AL1
X2=-L1-YB+I*AL1
A = T*AL1
IWY = IWY + ((OM1+OMEGA)*Y1*A/2.)
IWX = IWX + ((OM1*X1 +OMEGA*X2)*A/3.) + ( OM1*X2 + OMEGA*X1)*A/6.))
533 CONTINUE
C CALCULATE OMEGA SECTION 2
DO 550 I=1,K
OM1 = OMEGA
OMEGA=OMEGA+AL2*YB
T = T2
H =D2-I+1
ST = SA +SR2(H)
IF(ST.GE.SY)T = 0.
Y1=XAXIS-(I-1)*AL2
Y2=XAXIS-I*AL2
X1=-YB
A = T*AL2
IWX = IWX + (OM1+OMEGA)*X1*A/2.
IWY = IWY +(OM1*Y1 +OMEGA*Y2)*A/3. +(OM1*Y2 +OMEGA*Y1)*A/6.
550 CONTINUE
C CALCULATE LEG ADDITION
L=D2-K
OMLEG=OMEGA
IF(L.EQ.0.0)GO TO 1550
DO 1550 I=1,L
OM1=OMLEG
OMLEG=OMLEG+AL2*YB
T=T2
H=D2-K-I+1
ST=SA+SR2(H)
IF(ST.GE.SY)T=0.0
Y1=XAXIS-GUAGE-(I-1)*AL2
Y2=XAXIS-GUAGE-I*AL2
X1=-YB
A=T*AL2
IWX=IWX+(OM1+OMLEG)*X1*A/2.
IWY=IWY+(OM1*Y1 +OMLEG*Y2)*A/3. +(OM1*Y2+OMLEG*Y1)*A/6.
1550 CONTINUE
C CALCULATE OMEGA SECTION 3
DO 560 I=1,D3
OM1 = OMEGA
OMEGA = OMEGA + (AL3*(GUAGE-XAXIS))
T = T3
ST = SA +SR3(I)
IF(ST.GE.SY)T= .0
X1=-YB+(I-1)*AL3
X2=-YB+I*AL3
Y1 = (XAXIS-GUAGE)
A = T*AL3
IWY = IWY + ((OM1+OMEGA)*Y1*A/2.)
IWX = IWX + ((OM1*X1 +OMEGA*X2)*A/3.) + ( OM1*X2 + OMEGA*X1)*A/6.))
560 CONTINUE
C CALCULATE OMEGA SECTION 4
C CALCULATE LFG ADDITION
OMLEG=OMEGA
IF(L.EQ.0.0)GO TO 1560
DO 1560 I=1,L
OM1=OMLEG
OMLEG=OMLEG-AL2*YB
T=T2
H=D2-K-I+1
ST=SA+SR2(H)
IF(ST.GE.SY)T=0.0
Y1=XAXIS-GUAGE-(I-1)*AL2
Y2=XAXIS-GUAGE-I*AL2
X1=YB
A=T*AL2
IWX=IWX+(OM1+OMLEG)*X1*A/2.
IWY=IWY+(OM1*Y1+OMLEG*Y2)*A/3. +(OM1*Y2+OMLEG*Y1)*A/6.
1560 CONTINUE

```



```

AL4=AL2
DO 570 I=1,K
OM1=OMEGA
OMEGA=OMEGA+AL2*YB
T = T2
H=D2-K+I
ST = SA + SR2(H)
IF(ST.GE.SY)T=0.0
Y1 = XAXIS-GUAGE +(I-1)*AL4
Y2 = XAXIS - GUAGE + I*AL4
X1=YB
A = T*AL4
IWX = IWX + (OM1+OMEGA)*X1*A/2.
IWX = IWX + (OM1*Y1 +OMEGA*Y2)*A/3. + (OM1*Y2 +OMEGA*Y1)*A/6.
570 CONTINUE
C CORNER SECTION 5
DO 580 I=1,D1
OM1 = OMEGA
OMEGA=OMEGA-AL1*XAXIS
T = T1
H=D2-I+1
ST = SA +SR1(H)
IF(ST.GE.SY)T = 0.
Y1=XAXIS
X1=YB+(I-1)*AL1
X2=YB+I*AL1
A = T*AL1
IWX = IWX + ((OM1+OMEGA)*Y1*A/2.)
IWX = IWX + ((OM1*X1 +OMEGA*X2)*A/3.) + ( OM1*X2 + OMEGA*X1)*A/6.))
580 CONTINUE
WRITE(OUTPUT,532)OMEGA,IWX,IWX
532 FORMAT(10X,'OMEGA=',F10.4,8X,'IWX=',F8.4,10X,'IWX=',F8.4/)
534 FORMAT(10X,'##### END SECTION #####')
1532 FORMAT(10X,'OMLEG=',F10.4,8X,'IWX=',F8.4,10X,'IWX=',F8.4/)
1534 FORMAT(10X,'#####END LEG ADDITION #####')
C CALCULATE LOCATION OF SHEAR CENTRE(TORSIONAL CONSIDERATIONS)
XO = IWX/IXX
YO = -IWX/IYY
WRITE(OUTPUT,581)XO,YO
581 FORMAT(10X,'XO=',F10.4,10X,'YO=',F10.4/)
C CALCULATE WD SECTION 1 #####
NUM=1
OMEGA = 0.0
SN = 1.0
YYBAR = YBAR-YO
WRITE(OUTPUT,600)YYBAR
600 FORMAT(10X,'YYBAR=',F12.4/)
IF(YO.GE.YBAR)SN=-1.0
WO(1)=0.0
DO 602 I =1,D1
OMEGA=OMEGA-AL1*YYBAR*SN
NUM = NUM + 1
WO(NUM) = OMEGA
ST=SA+SR1(I)
IF(ST.GE.SY)ST=SY
STRESS=ST*F
Y1=YYBAR
X1=-L1-YB+(2*I-1)*AL1/2.
ADIST=X1**2+Y1**2
BARK=BARK+2.*STRESS*ADIST*AL1*T1
602 CONTINUE
C SECTION 2
DO 610 I =1,K
OMEGA=OMEGA+AL2*YB
NUM = NUM + 1
WO(NUM) = OMEGA
ST=SA+SR2(I)
IF(ST.GE.SY)ST=SY
STRESS=ST*F
Y1=YYBAR-(2*I-1)*AL2/2.
X1=YB
ADIST=X1**2+Y1**2
BARK=BARK+2.*STRESS*ADIST*AL2*T2
610 CONTINUE
WOLL=OMEGA
C CALCULATE WD LEG ADDITION
OMLEG=OMEGA
IF(L.FQ.0.0)GO TO 1610
DO 1610 I=1,L
OMLEG=OMLEG+AL2*YB
NUM=NUM+1
WO(NUM)=OMLEG
ST=SA+SR2(K+I)
IF(ST.GE.SY)ST=SY
STRESS=ST*F
Y1=YYBAR-GUAGE-(2*I-1)*AL2/2.
X1=YB
ADIST=Y1**2+X1**2
BARK=BARK+2.*STRESS*ADIST*AL2*T2
1610 CONTINUE

```



```

C SECTION 3
  SN = 1.0
  IF(YYBAR.GE.GUAGE)SN = -1.0
  KK=D3-1
  DO 620 I = 1, KK
    OMEGA = OMEGA + (AL3*ABS(GUAGE-YYBAR))*SN
    NUM = NUM + 1
    WO(NUM) = OMEGA
    ST=SA+SR3(I)
    IF(ST.GE.SY)ST=SY
    STRESS=ST*E
    Y1=YYBAR-GUAGE
    X1=YB-(2*I-1)*AL3/2.
    AOIST=Y1**2+X1**2
    BARK=BARK+STRESS*AOIST*AL3*T3
  620 CONTINUE
    OMEGA=OMEGA+AL3*ABS(GUAGE-YYBAR)*SN
    NUM = NUM + 1 + L
    WO(NUM) = OMEGA
C CALCULATE LEG ADDITION
  OMLEG=OMEGA
  IF(L.EQ.0.0)GO TO 1640
  DO 1640 I=1, L
    OMLEG=OMLEG-AL2*YB
    NUM=NUM-1
    WO(NUM)=OMLEG
  1640 CONTINUE
C SECTION 4
  NUM=NUM+L
  DO 630 I = 1, K
    OMEGA=OMEGA+AL2*YB
    NUM = NUM + 1
    WO(NUM) = OMEGA
  630 CONTINUE
C SECTION 5
  SN = 1.0
  IF(YO.GE.YBAR)SN=-1.0
  DO 640 I=1, O1
    OMEGA=OMEGA-AL1*YYBAR*SN
    NUM = NUM + 1
    WO(NUM) = OMEGA
  640 CONTINUE
  WRITE(OUTPUT,601) NUM, OMEGA
  601 FORMAT('O',10X,'WO(',I3,')=' ,F10.4)
C CALCULATE OMEGA (N)
C SECTION 1
  J=1
  OMEGN = 0.0
  WRITE(OUTPUT,701) J, OMEGN
  WN(1)=0.0
  DO 702 I = 1, O1
    T = T1
    ST = SA + SR1(I)
    IF(ST.GE.SY)T=0.0
    OMEGN=OMEGN+(WO(J)+WO(J+1))*T*AL1
    J = J + 1
    WN(J) = OMEGN
  702 CONTINUE
C SECTION 2
  DO 710 I=1, O2
    T = T2
    H = D2-I+1
    ST = SA + SR2(H)
    IF(ST.GE.SY)T=0.0
    OMEGN=OMEGN+(WO(J)+WO(J+1))*T*AL2
    J = J + 1
    WN(J) = OMEGN
  710 CONTINUE
C SECTION 3
  T = T3
  ST=SA+SR3(1)
  IF(ST.GE.SY)T=0.0
  OMEGN=OMEGN+(WO(1)+WO(J+1))*T*AL3
  J = J + 1
  WN(J) = OMEGN
  DO 720 I = 2, KK
    T = T3
    ST = SA + SR3(I)
    IF(ST.GE.SY)T=0.0
    OMEGN=OMEGN+(WO(J)+WO(J+1))*T*AL3
    J = J + 1
    WN(J) = OMEGN
  720 CONTINUE
    T = T3
    ST=SA+SR3(O3)
    IF(ST.GE.SY)T=0.0
    OMEGN=OMEGN+(WO(J)+WO(J+L+1))*T*(AL3)
    J=J+L+1
    WN(J) = OMEGN

```



```

C SECTION 4
  IF(L.EQ.0.0)GO TO 725
  DO 725 I=1,L
    T=T2
    H=L-I+1
    ST=SA+SR2(H)
    IF(ST.GE.SY)T=0.0
    OMEGN=OMEGN +(WO(J)+WO(J-1))*T*AL4
    J=J-1
    WN(J)=OMEGN
  725 CONTINUE
    J=J+L
    DO 730 I=1,K
      T = T2
      H=L+I
      ST = SA + SR2(H)
      IF(ST.GE.SY)T=0.0
      OMEGN=OMEGN+(WO(J)+WO(J+1))*T*AL4
      J = J + 1
      WN(J) = OMEGN
    730 CONTINUE
C SECTION 5
  DO 740 I=1,D1
    T = T1
    H=D1-I+1
    ST = SA + SR1(H)
    IF(ST.GE.SY)T=0.0
    OMEGN=OMEGN+(WO(J)+WO(J+1))*T*AL1
    J = J + 1
    WN(J) = OMEGN
  740 CONTINUE
    WRITE(OUTPUT,701)J,OMEGN
  701 FORMAT(10X,'WN(',I3,')=',F10.4//)
    AREA=YAREA
    OMEGAN=OMEGN/(AREA*2.)
C AREA CALCULATED ON REMAINING ELASTIC COPE
  WRITE(OUTPUT,741)OMEGAN,AREA
  741 FORMAT(10X,'OMEGAN=',F10.4,'AREA=',F10.4//)
C CALCULATE WNN
C WNN=W(N)/AREA
  SUM=0.0
  DO 802 I=1,J
    COR=WO(I)
    AWNN=OMEGAN-COR
    WNN(I)=AWNN
    SUM=SUM+WNN(I)
  802 CONTINUE
    WRITE(OUTPUT,801)I,WNN(I)
  801 FORMAT(10X,'WNN(',I3,')=',F10.4//)
C IF DISTRIBUTION OF PREVIOUS PROPERTIES OK SUM=0.0
  WRITE(OUTPUT,804)SUM
  804 FORMAT(10X,'SUM=',F10.6//)
C CALCULATE WARPING MOMENT OF INERTIA(IW)
C SECTION 1
  AAIW=0.0
  J=1
  DO 830 I=1,D1
    T=T1
    ST=SA+SR1(I)
    IF(ST.GE.SY)T=0.0
    AAIW=AAIW+((WNN(J)**2) + (WNN(J)*WNN(J+1))+(WNN(J+1)**2))*T*AL1
    J=J+1
    AIW(J)=AAIW
  830 CONTINUE
C SECTION 2
  T=T2
  DO 840 I=1,D2
    T=T2
    H=D2-I+1
    ST=SA+SR2(H)
    IF(ST.GE.SY)T=0.0
    AAIW=AAIW+((WNN(J)**2) + (WNN(J)*WNN(J+1))+(WNN(J+1)**2))*T*AL2
    J=J+1
    AIW(J)=AAIW
  840 CONTINUE
C SECTION 3
  T=T3
  ST=SA+SR3(1)
  IF(ST.GE.SY)T=0.0
  M=J-L
  AAIW=AAIW+((WNN(M)**2) + (WNN(M)*WNN(J+1))+(WNN(J+1)**2))*T*AL3
  J=J+1
  AIW(J)=AAIW
  DO 850 I=2,KK
    T=T3
    ST=SA+SR3(I)
    IF(ST.GE.SY)T=0.0
    AAIW=AAIW+((WNN(J)**2) + (WNN(J)*WNN(J+1))+(WNN(J+1)**2))*T*AL3
    J=J+1
    AIW(J)=AAIW
  850 CONTINUE

```



```

      T=T3
      ST=SA+SR3(D3)
      IF(ST.GE.SY)T=0.0
      N=J+L+1
      AAIW=AAIW+((WNN(J)**2) + (WNN(J)*WNN(N))+(WNN(N)**2))*T*AL3
      J=J+1
      AIW(J)=AAIW
C SECTION 4
      DO 860 I=1,D2
      T=T2
      H=D2-K+1
      ST=SA+SR2(H)
      IF(ST.GE.SY)T=0.0
      AAIW=AAIW+((WNN(J)**2) + (WNN(J)*WNN(J+1))+(WNN(J+1)**2))*T*AL2
      J=J+1
      AIW(J)=AAIW
860 CONTINUE
C SECTION 5
      DO 870 I=1,D1
      T=T1
      H=D1-I+1
      ST=SA+SR1(H)
      IF(ST.GE.SY)T=0.0
      AAIW=AAIW+((WNN(J)**2) + (WNN(J)*WNN(J+1))+(WNN(J+1)**2))*T*AL1
      J=J+1
      AIW(J)=AAIW
870 CONTINUE
      WRITE(OUTPUT,831)J,AAIW
831 FORMAT('O',10X,'IW(',I3,')=' ,F10.4)
      AIWW=AAIW/3.
      WRITE(OUTPUT,871)AIWW
871 FORMAT(10X,'IW OF SECTION=' ,F10.4//)
C CALCULATE VALUES FOR BUCKLING EQUATIONS
C NDTE (R0**2)=BARK/LOAD
      XA=E*IYY*3.14159*3.14159
      XB=LOAD
      XC=E*AIWW*3.14159*3.14159
      XD=G*AKT
      XE=BARK
      XF=(LOAD*YD)**2
      WRITE(OUTPUT,902)XA,XB,XC
      WRITE(OUTPUT,902)XD,XE,XF
902 FORMAT(10X,F14.4,3X,F14.4,3X,F14.4//)
C SET UP QUADRATIC FOR SOLUTION IN TERMS OF A CRITICAL LENGTH
C QUADRATIC ( AA(L**4) + BB(L**2) + CC = 0.0
      AA=-XB*XD-XB*XE-XF
      BB=XA*XD+XA*XE-XB*XC
      CC=XA*XC
      WRITE(OUTPUT,904)AA,BB,CC
904 FORMAT(10X,'A=' ,F14.4,3X,'B=' ,F14.4,3X,'C=' ,F14.4//)
      XAC=(BB*BB-4.*AA*CC)**0.5
      XX1=(-BB+XAC)/(2.*AA)
      XX2=(-BB-XAC)/(2.*AA)
      WRITE(OUTPUT,905)XX1,XX2
905 FORMAT(10X,F14.4,8X,F14.4//)
C CHECK FOR AN IMAGINARY SOLUTION
C XX1 AND XX2 REPRESENT SOLUTIONS
      IF(XX1.GE.0.0)LL1=XX1**0.5
      IF(XX2.GE.0.0)LL2=XX2**0.5
      WRITE(OUTPUT,900)LL1,LL2
900 FORMAT(10X,'CRITICAL LENGTH=' ,F10.4,8X,'OR=' ,F10.4,' INCHES'//)
      LOAD=0.0
      IXX=0.0
      IYY=0.0
      A=0.0
      AD=0.0
      GO TO 10
999 STOP
C SAMPLE DATA LAYOUT
C MODULUS OF ELASTICITY, YIELD STRESS, SHEAR MODULUS
C SECTION GEOMETRY AND NUMBER OF DIVISIONS FOR EACH LEG,GAUGE LOCATION
C RESIDUAL STRAIN FOR EACH DIVISION
C APPLIED STRAIN LEVEL(INCREMENT UNTIL SECTION FULLY YIELDED)
      END

```

ADCONS FOR EXTERNAL REFERENCES

***** END OF COMPILATION *****

B29959